

See discussions, stats, and author profiles for this publication at: <https://www.researchgate.net/publication/239730738>

# Structure–activity relationships of new cyanothiophene inhibitors of the essential peptidoglycan biosynthesis enzyme MurF

ARTICLE in EUROPEAN JOURNAL OF MEDICINAL CHEMISTRY · AUGUST 2013

Impact Factor: 3.45 · DOI: 10.1016/j.ejmech.2013.05.013

CITATIONS

7

READS

106

12 AUTHORS, INCLUDING:



**Martina Hrast**

University of Ljubljana

17 PUBLICATIONS 73 CITATIONS

SEE PROFILE



**Samo Turk**

BioMed X GmbH

45 PUBLICATIONS 372 CITATIONS

SEE PROFILE



**Izidor Sosič**

University of Ljubljana

27 PUBLICATIONS 132 CITATIONS

SEE PROFILE



**Hélène Barreteau**

Université Paris-Sud 11

31 PUBLICATIONS 561 CITATIONS

SEE PROFILE



## Original article

## Structure–activity relationships of new cyanothiophene inhibitors of the essential peptidoglycan biosynthesis enzyme MurF



Martina Hrast<sup>a</sup>, Samo Turk<sup>a</sup>, Izidor Sosič<sup>a</sup>, Damijan Knez<sup>a</sup>, Christopher P. Randall<sup>b</sup>,  
Hélène Barreteau<sup>c</sup>, Carlos Contreras-Martel<sup>d</sup>, Andréa Dessen<sup>d</sup>, Alex J. O'Neill<sup>b</sup>,  
Dominique Mengin-Lecreulx<sup>c</sup>, Didier Blanot<sup>c</sup>, Stanislav Gobec<sup>a,\*</sup>

<sup>a</sup> Faculty of Pharmacy, University of Ljubljana, Aškerčeva 7, 1000 Ljubljana, Slovenia

<sup>b</sup> Institute of Molecular and Cellular Biology and Antimicrobial Research Centre, University of Leeds, Leeds LS 9JT, UK

<sup>c</sup> Univ Paris-Sud, Enveloppes Bactériennes et Antibiotiques, IBBMC, UMR 8619 CNRS, 91405 Orsay, France

<sup>d</sup> Institut de Biologie Structurale, Bacterial Pathogenesis Group (CEA, CNRS, Université Grenoble I), 41 rue Jules Horowitz, 38027 Grenoble, France

## ARTICLE INFO

## Article history:

Received 15 February 2013

Received in revised form

10 May 2013

Accepted 13 May 2013

Available online 21 May 2013

## Keywords:

MurF inhibitors

Antibacterial agents

Crystal structures

## ABSTRACT

Peptidoglycan is an essential component of the bacterial cell wall, and enzymes involved in its biosynthesis represent validated targets for antibacterial drug discovery. MurF catalyzes the final intracellular peptidoglycan biosynthesis step: the addition of D-Ala-D-Ala to the nucleotide precursor UDP-MurNAc-L-Ala-γ-D-Glu-*meso*-DAP (or L-Lys). As MurF has no human counterpart, it represents an attractive target for the development of new antibacterial drugs. Using recently published cyanothiophene inhibitors of MurF from *Streptococcus pneumoniae* as a starting point, we designed and synthesized a series of structurally related derivatives and investigated their inhibition of MurF enzymes from different bacterial species. Systematic structural modifications of the parent compounds resulted in a series of nanomolar inhibitors of MurF from *S. pneumoniae* and micromolar inhibitors of MurF from *Escherichia coli* and *Staphylococcus aureus*. Some of the inhibitors also show antibacterial activity against *S. pneumoniae* R6. These findings, together with two new co-crystal structures, represent an excellent starting point for further optimization toward effective novel antibacterials.

© 2013 Elsevier Masson SAS. All rights reserved.

## 1. Introduction

Infectious diseases represent the second major cause of death globally [1]. Although numerous antibacterial agents are currently available, their extensive and sometimes inappropriate use has resulted in the development of bacterial resistance [2,3]. Therefore, intensive research toward the development of new antibacterial agents with novel mechanisms of action has become an urgent need [4].

The enzymes involved in peptidoglycan biosynthesis rank among the best known and most extensively validated antibacterial

drug targets [5,6]. Peptidoglycan is an essential component of the bacterial cell wall, and its main function is the preservation of cell integrity by withstanding the internal osmotic pressure. It also helps to retain the characteristic shape of the bacterial cell, and protects the cell content from environmental factors. Peptidoglycan is composed of repeating disaccharide units of *N*-acetyl muramic acid (MurNAc) and *N*-acetyl glucosamine (GlcNAc) that are cross-linked by peptide chains [5,7–9]. Although the extracellular stages of cell wall biosynthesis are well exploited as drug targets and are inhibited by several therapeutically used drugs, such as the β-lactams and glycopeptide antibiotics [5], the intracellular stages remain underexploited. Only two currently used drugs act at the stage of cytoplasmic precursor formation: fosfomycin, which acts as an inhibitor of MurA, and D-cycloserine, which inhibits both alanine racemase and D-alanine:D-alanine ligase [10,11].

The Mur ligases (MurC, MurD, MurE and MurF) are intracellular ATP-dependent enzymes that share similar reaction mechanisms and three-dimensional structures [12,13]. They catalyze the sequential addition of L-Ala, D-Glu, *meso*-DAP or L-Lys, and the dipeptide D-Ala-D-Ala to UDP-MurNAc, to form UDP-MurNAc-pentapeptide. In most Gram-negative bacteria, mycobacteria and

**Abbreviations:** DAP, 2,6-diaminopimelic acid; GlcNAc, *N*-acetyl glucosamine; MurC, UDP-*N*-acetylmuramate:L-Ala ligase; MurD, UDP-*N*-acetylmuramoyl-L-Ala:D-Glu ligase; MurE, UDP-*N*-acetylmuramoyl-L-Ala-D-Glu:*meso*-DAP ligase or L-Lys; MurF, UDP-*N*-acetylmuramoyl-L-Ala-γ-D-Glu-*meso*-DAP (or L-Lys):D-Ala-D-Ala ligase; MurNAc, *N*-acetyl muramic acid; UDP, uridine 5'-diphosphate; UMtri-L-Lys, UDP-*N*-acetylmuramoyl-L-Ala-D-Glu-L-Lys; UMtri-mDAP, UDP-*N*-acetylmuramoyl-L-Ala-γ-D-Glu-*meso*-DAP.

\* Corresponding author. Tel.: +386 1 4769500; fax: +386 1 4258031.

E-mail address: [stanislav.gobec@ffa.uni-lj.si](mailto:stanislav.gobec@ffa.uni-lj.si) (S. Gobec).

bacilli, MurF catalyzes the addition of D-Ala-D-Ala to the nucleotide precursor UDP-MurNac-L-Ala-γ-D-Glu-*meso*-diaminopimelate (UMtri-mDAP). In Gram-positive bacteria, the nucleotide precursor contains L-Lys instead of *meso*-DAP [7,14,15]. MurF has been recognized as essential for the growth of bacteria [16–18], and its active site is highly conserved in all medically important pathogens [19]. As MurF has no human counterpart, it represents an attractive target for the development of new antibacterial drugs.

The first reported MurF inhibitors were pseudo-tripeptide and pseudo-tetrapeptide aminoalkylphosphinate mimetics of the transition state, with  $K_i$  values ranging from 200 μM to 700 μM [20]. The sulfonamide inhibitors (e.g., Fig. 1: **1**) were discovered by Abbott Laboratories, using affinity selection screening technology [21], and they were co-crystallized with the enzyme [16]. The subsequent structure-based optimization led to highly potent nanomolar inhibitors (e.g. **2**) [22,23]. A mucopeptide-ligase-based assay was used to identify the thiazolylaminopyrimidine series of MurF inhibitors with  $IC_{50}$  values as low as 2.5 μM (e.g. **3**) [19]. The crystal structure of *Streptococcus pneumoniae* MurF (PDB code 2AM1) [16] was also used for structure-based virtual screening, which identified a novel MurF inhibitor **4** [24]. Furthermore, a series of 8-hydroxyquinolines was found to inhibit *Escherichia coli* MurF; this series was later used as the basis for pharmacophore modeling, to identify additional inhibitors without chelating properties [25]. Two structurally different classes of inhibitors were discovered as well; namely, the 4-phenylpiperidine derivatives and the diarylquinolines (**5**) [26]. However, most of these inhibitors lack good antibacterial activities, most likely due to the poor cell permeability, with the exception of the 4-phenylpiperidine derivatives and diarylquinolines that show modest antibacterial activity against *E. coli* (MIC values 8–16 μg/mL) [26].

We present here the design, synthesis, biological evaluation and co-crystallization of a new series of cyanothiophene-based inhibitors of MurF enzymes from different pathogenic bacteria. The design of these compounds was based on previously published inhibitors (**1** and **2**) [22,23]. Systematic structural modifications of these lead compounds resulted in a comprehensive series of new inhibitors, providing nanomolar inhibitors of *S. pneumoniae* MurF (MurF<sub>Sp</sub>) and micromolar inhibitors of MurF of *E. coli* (MurF<sub>Ec</sub>) and *Staphylococcus aureus* (MurF<sub>Sa</sub>). These structural optimizations represent an important development of MurF inhibitors toward potential antibacterial drugs.

## 2. Results and discussion

### 2.1. Design

It is known from the Abbott Laboratories series of compounds that 2-aminothiophene-3-carbonitrile and 5-sulfamoyl-2-chloro benzoic acid linked together via an amide bond are essential for good inhibitory activity (Fig. 2). The introduction of 4-chlorine to the benzoic acid resulted in even greater potency [16,22]. However, the greatest increase in potency was achieved when an aryl group was attached to position 6 of the 4,5,6,7-tetrahydrobenzo[*b*]thiophene ring. These structural modifications led to compounds with 14-fold to 45-fold improved potencies compared to **1** [23].

Due to its good MurF inhibitory activity and appropriate molecular mass, we initiated systematic structural modifications of lead compound **1**, as illustrated in Fig. 2. First, various sulfonamides were synthesized to examine the inhibitory potency of compounds with different replacements of the morpholino group (Fig. 2: variations of substituent R<sup>1</sup>). Furthermore, different substituents were attached to position 6 of the 4,5,6,7-tetrahydrobenzo[*b*]thiophene core (Fig. 2: variations of substituent R<sup>2</sup>), as it is known that extension of this ring system at position 6 leads to greater potency [23]. Given that the fused 4,5,6,7-tetrahydrobenzo ring is not essential for biological activity and can be replaced by other rings [22,23], 4,5,6,7-tetrahydrothieno[2,3-*c*]pyridine was introduced, which allows for rapid introduction of *N*-phenyl, -benzyl and -alkyl substituents at position 6 and enabled the synthesis of a comprehensive series of compounds to study the structure–activity relationships (SARs).

### 2.2. Chemistry

The synthesis of the fused 2-aminothiophenes **9a–g** (Table 1), the crucial building blocks for all of the target compounds, is presented in Scheme 1. The synthesis was performed via different cyclic ketones (Scheme 1: **8a–c**, **10**, **12e–f**, **14**) that were either commercially available (such as cyclohexanone (**10**)) or were synthesized, as follows (Scheme 1):

- (i) The synthesis of 1-phenylpiperidin-4-ones (**8a–c**) involved the displacement of fluorine from activated aryl fluorides with 4-piperidone ethylene acetal (**6**) in the presence of sodium

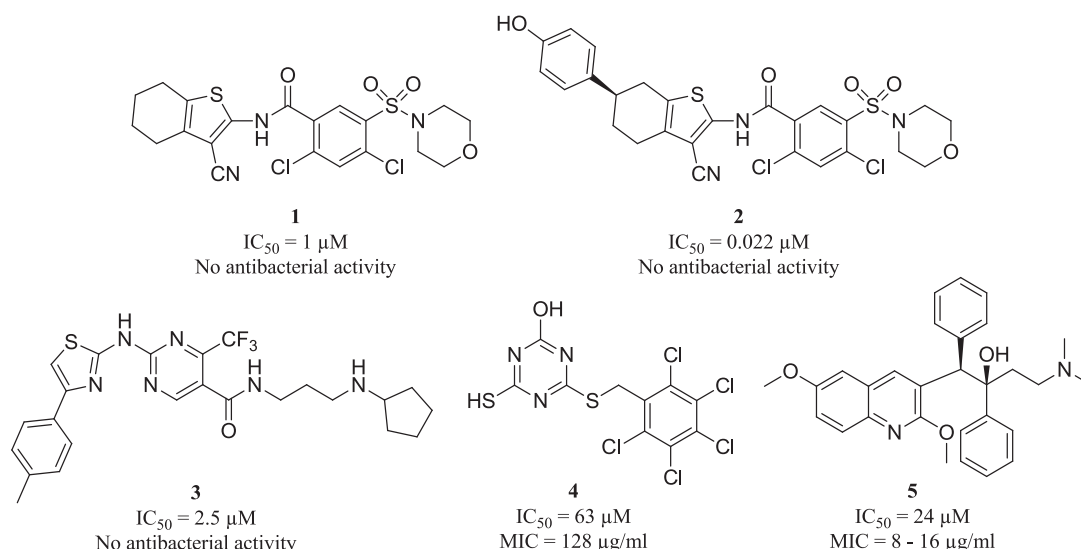
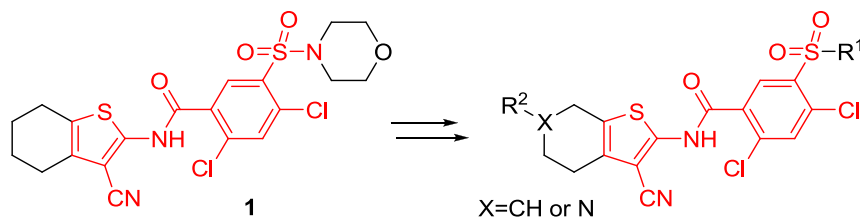


Fig. 1. Structural formulas of the known MurF inhibitors, with their corresponding inhibitory and antimicrobial activities.



**Fig. 2.** A typical MurF<sub>Sp</sub> inhibitor. Groups essential for inhibitory activity are shown in red. (For interpretation of the references to color in this figure legend, the reader is referred to the web version of this article.)

carbonate in DMSO, yielding compounds **7a–c**. This was followed by mild acidic hydrolysis (10% H<sub>2</sub>SO<sub>4</sub> in THF) of the acetal protective group.

- (ii) The hydroxyl group of **11** was converted into the methoxy moiety using iodomethane, via Williamson synthesis of ethers, or acetylated with acetic anhydride in pyridine, yielding compounds **12e–f**.
- (iii) 4-Oxopiperidine hydrochloride (**13**) was reacted with di-*tert*-butyl dicarbonate ((Boc)<sub>2</sub>O) under aqueous conditions in the presence of TEA, to give the Boc-protected compound **14**. Finally, 2-aminothiophenes (**9a–g**) were obtained via three component condensation between sulfur, cyclic ketone and malononitrile in the presence of morpholine as a base, using the Gewald reaction.

The synthesis of target compounds **18a–n**, **19d–e** and **20** is presented in Scheme 2. In the first step, 2,4-dichlorobenzoic (**15**) acid was chlorosulfonated, to yield the sulfonyl chloride (**16**) that was subsequently reacted with different secondary amines to give the various sulfonamides (**17a–h**). These were coupled with 2-aminothiophenes (**9a–g**) via a two-stage process, involving the conversion of the acid into acyl chloride in the presence of oxalyl chloride and catalytic amounts of DMF, followed by the coupling in the presence of pyridine as a base, to give **18a–n**. As far as carboxylate esters **18d–e** are concerned, their hydrolysis with KOH provided **19d–e**. Finally, compound **20** was obtained by the reduction of the keto group of **18f** with sodium borohydride.

**Table 1**  
Different substituents applied to the saturated ring (Fig. 2: R<sup>2</sup>).

Compound	X	R <sup>2</sup>
<b>9a</b>	N	
<b>9b</b>	N	
<b>9c</b>	N	
<b>9d</b>	CH <sub>2</sub>	/
<b>9e</b>	CH	
<b>9f</b>	CH	
<b>9g</b>	N	Boc

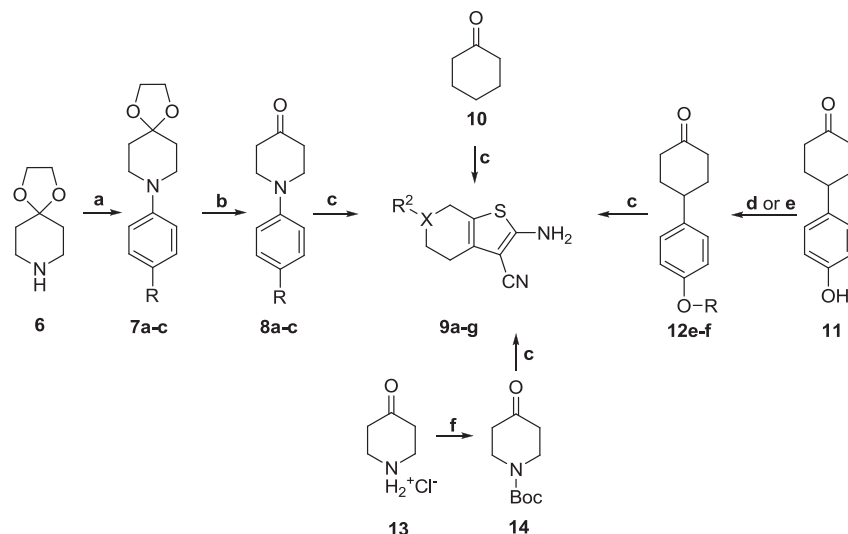
Compounds **21**, **22a–w** and **23–25** were synthesized as outlined in Scheme 3. The Boc protective group of compound **18i** was cleaved under anhydrous conditions in the presence of CF<sub>3</sub>COOH or HCl in ethanol, to obtain **21**. The variously substituted benzyl or alkyl fragments were then attached to the main scaffold via two different strategies. The first method was a classical nucleophilic substitution reaction, where K<sub>2</sub>CO<sub>3</sub> and different benzyl or alkyl bromides were used to obtain compounds **22a–h**; in the second method, compounds **22i–w** were synthesized by reductive amination of **21** with a variety of benzaldehydes, using sodium triacetoxyborohydride as the reducing agent and CH<sub>3</sub>COOH as the catalyst. The formation of the amide **23** was achieved with the coupling of benzoyl chloride and **21** in the presence of TEA. Compound **24** was obtained by the cleavage of the Boc protective group of **22a**, whereas the removal of the acetyl groups of **22q** with sodium methoxide yielded compound **25**.

### 2.3. Biological activity

Target compounds **18a–n**, **19d–e**, **20**, **21**, **22b–w** and **23–25** (Schemes 2 and 3) were tested for their inhibitory activities on MurF<sub>Sp</sub>, MurF<sub>Ec</sub> and MurF<sub>Sa</sub> using the Malachite green assay [27]. To exclude possible non-specific inhibition, all of the compounds were tested in the presence of detergent (0.005% Triton X-114) [28]. The results are presented as residual activities (RAs) of the respective MurF in the presence of 100 μM of each compound. For the compounds with RAs lower than 50%, the IC<sub>50</sub> values were also determined. To confirm the suitability of the MurF<sub>Sp</sub> inhibition assay, and for a better comparison of newly synthesized compounds with known inhibitors, Abbott inhibitor **1** (Figs. 1 and 2) was re-synthesized. Compound **1** was 4-fold less potent in our assay as compared with the published activity (IC<sub>50</sub> = 4 μM versus 1 μM), which can be attributed to the different assay conditions [22].

### 2.4. Structure–activity relationships: the influence of different R<sup>1</sup> substituents

With the intention of further exploring the SARs of these compounds, a focused library of compound **1** analogs was synthesized where the morpholine moiety was replaced by different saturated heterocycles (Scheme 2; Table 2: compounds **18a–h**, **19d–e**, **20**). The thiomorpholine (**18a**), thiazolidine (**18b**) and 3-oxopiperazine (**18c**) derivatives showed significantly lower inhibition of MurF<sub>Sp</sub> than parent compound **1**, most likely due to the introduction of the bulky sulfur atom in **18a** and **18b**, or to the increased rigidity of the ring in **18c**. Most of the compounds with the piperidine moiety (**18d–e**, **18h**, **19d–e**, **20**) were inactive or less active than compound **1**. The introduction of a carboxyethyl group in the *meta* (**18d**) or *para* (**18e**) position led to a decrease in potency; however, the carboxylic derivatives (**19d–e**) showed modest inhibitory activities. The *p*-methylpiperidine derivative (**18h**) completely lost the inhibition, although compound **18g** with a methyl group in the *ortho* position on the piperidine ring showed very promising activity



**Scheme 1.** Reagents and conditions: (a)  $\text{Na}_2\text{CO}_3$ , aryl fluoride, DMSO,  $120^\circ\text{C}$ , 16 h; (b)  $\text{H}_2\text{SO}_4$ , THF, rt, 48 h; (c) **8** or **10** or **12** or **14**, S,  $\text{CNCH}_2\text{CN}$ , morpholine, EtOH, reflux, 2 h; (d)  $\text{Cs}_2\text{CO}_3$ , MeI, acetone, reflux, 1 h; (e)  $\text{Ac}_2\text{O}$ , pyridine, rt, 18 h; (f)  $(\text{Boc})_2\text{O}$ , TEA, rt, 16 h.

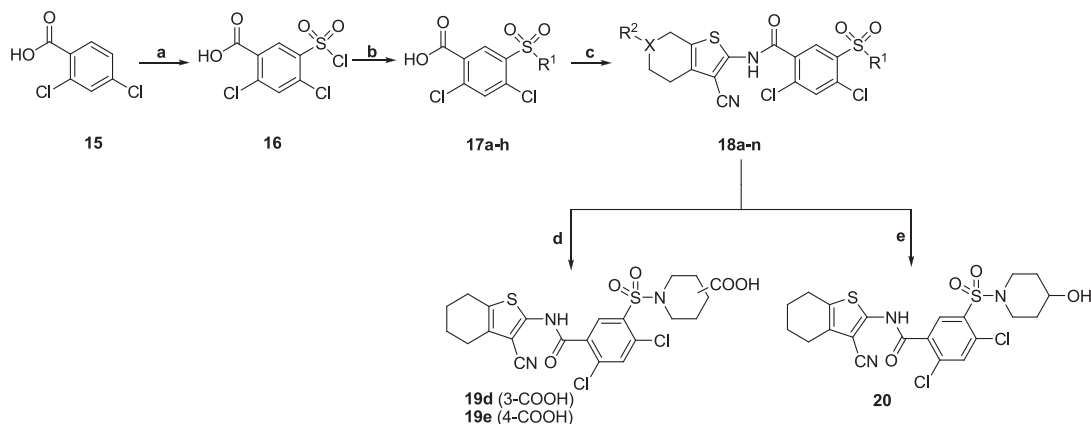
( $\text{IC}_{50} = 3.75 \mu\text{M}$ ), as comparable to compound **1**. Compound **20**, with a *p*-hydroxyl group, was only 2.5-fold less potent than **1**; however compound **18f** with a carbonyl function at the *para* position again showed a comparable activity ( $\text{IC}_{50} = 3.37 \mu\text{M}$ ) to **1**. All of these sulfonamide analogs were also assayed for inhibition of  $\text{MurF}_{\text{Ec}}$  and  $\text{MurF}_{\text{Sa}}$ , and they were inactive against both of these enzymes.

### 2.5. Structure–activity relationships: the influence of different $R^2$ substituents

A number of compounds (Table 3) were prepared to examine the influence on MurF inhibition of different 6-substituents attached to either the 4,5,6,7-tetrahydrobenzo[*b*]thiophene-3-carbonitrile or the 4,5,6,7-tetrahydrothieno[2,3-*c*]pyridine-3-carbonitrile core. The most potent inhibitors of  $\text{MurF}_{\text{Sp}}$  were compounds **18j–k** with *p*-methoxy and *p*-acetoxyphenyl rings attached to the fused 4,5,6,7-tetrahydrobenzene ring at position 6. They were 33-fold and 23-fold more potent than the parent compound **1**, with  $\text{IC}_{50}$  values of  $0.12 \mu\text{M}$  and  $0.17 \mu\text{M}$ , respectively. However, neither of these two compounds showed inhibitory activity against  $\text{MurF}_{\text{Ec}}$  and  $\text{MurF}_{\text{Sa}}$ . The compounds with phenyl substituents in

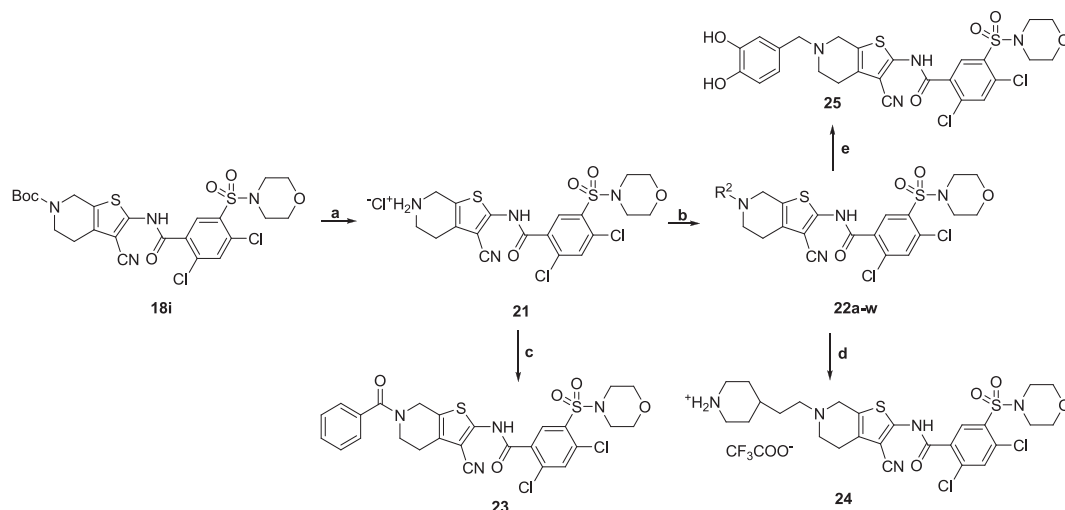
position 6 of the 4,5,6,7-tetrahydrothieno[2,3-*c*]pyridine ring (**18l–n**) showed no inhibition of any of these MurF enzymes, most likely due to differences in the conformation between the 4,5,6,7-tetrahydrobenzo[*b*]thiophene and 4,5,6,7-tetrahydrothieno[2,3-*c*]pyridine rings. Compound **23**, with a benzoyl group, showed moderate inhibitory activity of  $\text{MurF}_{\text{Sp}}$  ( $\text{IC}_{50} = 27 \mu\text{M}$ ), but was devoid of  $\text{MurF}_{\text{Ec}}$  and  $\text{MurF}_{\text{Sa}}$  inhibition. Inhibitor **24** showed good inhibitory activity against  $\text{MurF}_{\text{Sp}}$ , with an  $\text{IC}_{50}$  of  $0.60 \mu\text{M}$ , but was also inactive against the other two MurF enzymes.

Finally, a series of inhibitors containing different benzyl substituents at position 6 were synthesized, and all of these showed promising inhibitory activities against all of these MurF enzymes. The 6-benzyl derivative **22c** and its saturated derivative **22b** with a 6-cyclohexylmethyl substituent were both potent inhibitors of  $\text{MurF}_{\text{Sp}}$  ( $\text{IC}_{50}$  values of  $0.64 \mu\text{M}$  and  $0.46 \mu\text{M}$ , respectively), most likely due to the same hydrophobic interaction pattern between the inhibitor and the enzyme; **22b** was, however, less potent on  $\text{MurF}_{\text{Ec}}$  and  $\text{MurF}_{\text{Sa}}$ . A general conclusion can be made for the benzyl-substituted derivatives **22c–w**: electron withdrawing groups substituted at the *para* or *meta* positions of the benzyl ring (compounds **22d–h** and **22j–l**) only slightly reduced the inhibitory activity against  $\text{MurF}_{\text{Sp}}$  compared to **22c**, while electron donating



**Scheme 2.** Reagents and conditions: (a)  $\text{HSO}_3\text{Cl}$ ,  $140^\circ\text{C}$ , 16 h; (b) corresponding secondary amine, TEA,  $\text{CH}_2\text{Cl}_2$ ,  $0^\circ\text{C}$  to rt, 16 h; (c) **1**,  $(\text{COCl})_2$ , DMF,  $\text{CH}_2\text{Cl}_2$ ,  $0^\circ\text{C}$  to rt, 1 h; **2**, **9a–g**, pyridine,  $\text{CH}_2\text{Cl}_2$ ,  $0^\circ\text{C}$  to rt, 16 h; (d) **18d** or **18e**, KOH, dioxane/water, rt, 2 h; (e) **18f**,  $\text{NaBH}_4$ , ethanol/ $\text{CH}_2\text{Cl}_2$ , rt, 3 h.





**Scheme 3.** Reagents and conditions: (a) HCl, EtOH, rt, 18 h or CF<sub>3</sub>COOH, CH<sub>2</sub>Cl<sub>2</sub>, rt, 2 h; (b) A: K<sub>2</sub>CO<sub>3</sub>, corresponding benzyl bromide, DMF, rt, 16 h; B: corresponding benzaldehyde, Na(OAc)<sub>3</sub>BH, AcOH, THF, rt, 16 h; (c) benzoyl chloride, TEA, CH<sub>2</sub>Cl<sub>2</sub>, rt, 16 h; (d) **22a**, TFA, CH<sub>2</sub>Cl<sub>2</sub>, rt, 2 h; (e) **22q**, 30% NaOMe, THF/MeOH, rt, 0.5 h.

groups (compounds **22i**, **22n** and **22o**) improved the inhibition by more than 3-fold. The only exception to this rule was compound **22m**, which was 2-fold more potent than the parent compound **22c**. In addition, if we compare compound **22k** with **22i** and compound **22n** with **22o**, it appears that *para* substitution was more favorable than the *meta* substitution. The bioisosteric replacement of the carboxylic group of **22k** with a more bulky and less acidic tetrazole group (**22m**) led to a 2.5-fold improvement in the inhibitory activity ( $IC_{50}$  = 0.32  $\mu$ M). The compounds with two or more substituents on the benzyl ring were mostly less potent than compound **22c**. The exception was compound **25**, with two OH groups positioned at the *para* and *meta* sites of the benzyl ring, which showed a comparable inhibitory activity to **22c** with an  $IC_{50}$  of 0.43  $\mu$ M. Here, the replacement of the *para* OH group with the methoxy moiety led to the similarly active compound **22s** ( $IC_{50}$  = 0.60  $\mu$ M). The substitution of the *meta* hydroxyl with a carboxy (**22w**) or methoxy (**22r**) moiety resulted in 3-fold and 10-fold lower activities, respectively. The replacement of both OH groups with acetoxy (**22q**) and methoxy (**22r**) moieties resulted in significantly lower inhibitory activities. The most promising inhibitor within this series was compound **22n**, with an  $IC_{50}$  of 0.18  $\mu$ M.

Most of the compounds from this series demonstrated moderate inhibitory activities for both MurF<sub>Ec</sub> and MurF<sub>Sa</sub> ( $IC_{50}$  values ca. 100  $\mu$ M). The most potent inhibitor of MurF<sub>Ec</sub> and MurF<sub>Sa</sub> was compound **22r**, with  $IC_{50}$  values of 37  $\mu$ M and 67  $\mu$ M, respectively. Interestingly, compound **22n**, with the 6-(*p*-hydroxybenzyl) substituent, and which was the best inhibitor of MurF<sub>Sp</sub> within this series, showed very low inhibitory activity against the orthologs from *E. coli* and *S. aureus*. However, inhibitor **22o**, with the 6-(*m*-hydroxybenzyl) substituent, and which possessed good inhibitory activity against MurF<sub>Sp</sub> ( $IC_{50}$  = 0.42  $\mu$ M), showed promising inhibition of MurF<sub>Ec</sub> and MurF<sub>Sa</sub> ( $IC_{50}$  values of 81  $\mu$ M and 91  $\mu$ M, respectively).

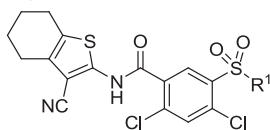
The differences in the inhibitory activities of these compounds on these different MurF ligases from different species were not surprising given that MurF<sub>Sp</sub> shows only 33% and 27% sequence identity with MurF<sub>Sa</sub> and MurF<sub>Ec</sub>, respectively. MurF<sub>Sa</sub> and MurF<sub>Ec</sub> themselves share 33% amino-acid sequence identity. These differences among the orthologs are further underlined by their different substrate selectivities. A closer look at the active sites of all three MurF enzymes reveals important differences among them

(Supporting information – Figure S1). Because of the specific MurF<sub>Sa</sub> and MurF<sub>Ec</sub> variations in the active site, several important interactions with cyanothiophene inhibitors are lost, leading to lower activity on both enzymes. It thus appears most probable that this type of cyanothiophene inhibitors of MurF have the potential to be developed into species-specific antibacterial agents for the treatment of infections with *S. pneumoniae*.

## 2.6. Crystal structures of MurF<sub>Sp</sub> in complex with compounds **22m** and **22n**

The crystal structures of MurF<sub>Sp</sub> in complex with compounds **22m** and **22n** were solved to 1.9 and 3 Å resolution (PDB codes 3zm6 and 3zm5), respectively, to determine the binding mode of the inhibitors within the active site of the enzyme. The data were collected at the European Synchrotron Radiation Facility (Grenoble, France), and the structures of the complexes were solved by molecular replacement using the known structure of complex of MurF<sub>Sp</sub> (PDB code 2AM1) [16].

Considering the similarity of our compound with Abbott inhibitors [22], there is no surprise that the co-crystals are in closed conformation and that the interaction pattern is similar to the one described before [16]. However, our crystal structures revealed new conformations of cyanothiophene inhibitors and disclosed some new interactions (Fig. 3). We found that the morpholino ring could occupy either chair (**22m**) or boat (**22n**) conformation. One of the sulfonyl oxygen atoms from the sulfonamide linker is in a position that allows it to make two hydrogen bonds, one with N<sup>δ</sup> from the side chain of Asn326, and one with N<sup>δ</sup> from the side chain of Asn328. The central benzene ring is held in place by  $\pi$ – $\pi$  interactions with Phe31. The chlorine next to sulfonamide linker forms hydrophobic interactions with Ile139 and the chlorine ortho to the amide linker forms the same type of interaction with Leu45. The amine group from amide is hydrogen bonded to the hydroxyl group of the side chain of Thr330. The nitrile group from the 3-cyanothiophene ring forms hydrogen bonds with the backbone of Arg49 and Ala48. Furthermore, the piperidine ring condensed with the cyanothiophene moiety makes hydrophobic interaction with side chains of residues Pro329, Leu360, Leu367 and Phe54. Finally, the new fragment in the molecules, the *p*-substituted benzyl ring, contributes to the recognition in the active site by forming the  $\pi$ – $\pi$  interactions with Phe54 and

**Table 2**Inhibitory activities of compounds **1**, **18a–h**, **19d–e** and **20** against MurF, and their antibacterial activities against *S. pneumoniae*.

Compound	R <sup>1</sup>	RA <sup>a</sup> (%) or IC <sub>50</sub> <sup>b</sup> (μM) MurF <sub>Sp</sub>	RA <sup>a</sup> (%) MurF <sub>Ec</sub>	RA <sup>a</sup> (%) MurF <sub>Spa</sub>	MIC (μg/mL) <i>S. pneumoniae</i>
<b>1</b>		4 μM	100	107	64
<b>18a</b>		42%	91	95	>128
<b>18b</b>		66%	104	85	>128
<b>18c</b>		89%	91	95	n.d.
<b>18d</b>		131 μM	94	93	n.d.
<b>18e</b>		100%	95	100	n.d.
<b>18f</b>		3.37 μM	102	103	>128
<b>18g</b>		3.75 μM	107	103	>128
<b>18h</b>		90%	87	80	n.d.
<b>19d</b>		50 μM	100	102	>128
<b>19e</b>		17.9 μM	102	96	64
<b>20</b>		10.45 μM	104	101	64

n.d., antibacterial activity not determined.

<sup>a</sup> Residual activity (%) of the enzyme at 100 μM of the tested compound. Data are means of two independent experiments. Standard deviations were within ±10% of the mean.<sup>b</sup> Concentration of the inhibitor for which the residual activity of the enzyme is 50%.

making the hydrophobic interaction with Arg34 and Leu360. The tetrazole moiety from compound **22m** is additionally hydrogen-bonded to carboxyl group of Asp362, while the hydroxyl group of compound **22n** forms the hydrogen bonds with the side chain carboxyl group of Asp362 and O<sup>δ</sup> of Gln363.

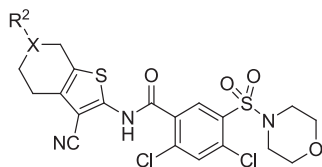
### 2.7. Antibacterial activity

The antibacterial activities of selected compounds were determined against *E. coli*, *S. aureus* and *S. pneumoniae*. None of the compounds tested demonstrated useful activity against *E. coli* (including efflux-deficient strains, or those in which the outer membrane had been artificially permeabilised) or *S. aureus*; this was as expected, as none of these compounds showed potent

inhibition of MurF<sub>Ec</sub> and MurF<sub>Spa</sub> *in vitro*. However, some of the compounds showed moderate antibacterial activity against *S. pneumoniae* (Tables 2 and 3). The compounds within the first series of inhibitors with the morpholino group (**1**) and their analogs (**19e**, **20**) prevented the growth of *S. pneumoniae* at a concentration of 64 μg/mL, while compounds **22p**, **22o** and **22v** showed the best activities, with MICs of 16 μg/mL to 32 μg/mL.

### 3. Conclusions

We have designed, synthesized and evaluated a comprehensive series of cyanothiophene-based inhibitors of the MurF enzymes from important pathogenic species: *S. pneumoniae*, *E. coli* and *S. aureus*. Systematic structural modifications of the lead compound

**Table 3**Inhibitory activities of compounds **18i–n**, **21**, **22b–w** and **23–25** against the MurF enzymes, and their antibacterial activity against *S. pneumoniae*.

Compound	X	R	RA <sup>a</sup> (%) or IC <sub>50</sub> <sup>b</sup> (μM) MurF <sub>Sp</sub>	RA (%) or IC <sub>50</sub> (μM) MurF <sub>Ec</sub>	RA (%) or IC <sub>50</sub> (μM) MurF <sub>Sa</sub>	MIC (μg/mL) ( <i>S. pneumoniae</i> )
<b>1</b>	CH	H	4 μM	100	107	64
<b>18i</b>	N		19 μM	88%	78%	128
<b>18j</b>	C		0.12 μM	91%	103%	>128
<b>18k</b>	C		0.17 μM	90%	85%	>128
<b>18l</b>	N		80%	98%	79%	>128
<b>18m</b>	N		63%	95%	85%	>128
<b>18n</b>	N		80%	74%	83%	>128
<b>21</b>	N	H <sub>2</sub> Cl <sup>−</sup>	47 μM	94%	81%	128
<b>22a</b>	N		n.d.	n.d.	n.d.	n.d.
<b>22b</b>	N		0.46 μM	63%	64%	>128
<b>22c</b>	N		0.64 μM	109 μM	80 μM	>128
<b>22d</b>	N		0.98 μM	100 μM	79 μM	>128
<b>22e</b>	N		1.92 μM	58%	92 μM	>128
<b>22f</b>	N		1.17 μM	99 μM	90 μM	>128
<b>22g</b>	N		1.36 μM	62 μM	80 μM	>128
<b>22h</b>	N		1.09 μM	101 μM	94 μM	128
<b>22i</b>	N		0.60 μM	82 μM	95 μM	>128

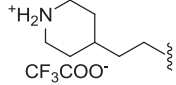
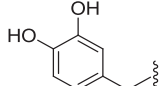


Table 3 (continued)

Compound	X	R	RA <sup>a</sup> (%) or IC <sub>50</sub> <sup>b</sup> (μM) MurF <sub>Sp</sub>	RA (%) or IC <sub>50</sub> (μM) MurF <sub>Ec</sub>	RA (%) or IC <sub>50</sub> (μM) MurF <sub>Sa</sub>	MIC (μg/mL) ( <i>S. pneumoniae</i> )
22j	N		0.72 μM	59 μM	88 μM	>128
22k	N		0.86 μM	118 μM	110 μM	>128
22l	N		2.55 μM	67 μM	118 μM	>128
22m	N		0.30 μM	55 μM	120 μM	>128
22n	N		0.18 μM	68%	84%	>128
22o	N		0.42 μM	81 μM	91 μM	16
22p	N		2.75 μM	81%	79%	32
22q	N		3.03 μM	88 μM	89 μM	>128
22r	N		10.4 μM	37 μM	66.5 μM	>128
22s	N		0.60 μM	77 μM	115 μM	>128
22t	N		4.15 μM	98 μM	64%	>128
22u	N		0.99 μM	73 μM	109 μM	>128
22v	N		48 μM	78 μM	84 μM	16
22w	N		1.41 μM	106 μM	132 μM	>128
23	N		27 μM	93%	107%	>128

(continued on next page)

Table 3 (continued)

Compound	X	R	RA <sup>a</sup> (%) or IC <sub>50</sub> <sup>b</sup> ( $\mu$ M) MurF <sub>Sp</sub>	RA (%) or IC <sub>50</sub> ( $\mu$ M) MurF <sub>Ec</sub>	RA (%) or IC <sub>50</sub> ( $\mu$ M) MurF <sub>Sa</sub>	MIC ( $\mu$ g/mL) ( <i>S. pneumoniae</i> )
24	N		0.60 $\mu$ M	93%	84%	>128
25	N		0.43 $\mu$ M	78%	64%	>128

n.d., antibacterial activity not determined.

<sup>a</sup> Residual activity (%) of the enzyme at 100  $\mu$ M of the tested compound. Data are means of two independent experiments. Standard deviations were within  $\pm 10\%$  of the mean.

<sup>b</sup> Concentration of the inhibitor for which residual activity of the enzyme is 50%.

resulted in new potent nanomolar inhibitors of MurF<sub>Sp</sub> and micromolar inhibitors of MurF<sub>Ec</sub> and MurF<sub>Sa</sub>. Two new co-crystal structures were obtained and they provide important information for future structure-based design of improved inhibitors. Some of the compounds showed moderate antibacterial activity against *S. pneumoniae*, and thus represent a good basis for further optimization toward an effective novel antibacterial drug.

## 4. Experimental section

### 4.1. Inhibition assay

The compounds were tested for inhibition of the addition of D-Ala-D-Ala to either UMtri-L-Lys or UMtri-mDAP catalyzed by MurF<sub>Sp</sub>, MurF<sub>Ec</sub> or MurF<sub>Sa</sub>. This assay was also based on the Malachite green method described above, with slight modifications, using a mixture (final volume, 50  $\mu$ L) containing:

#### 4.1.1. *S. pneumoniae* MurF

50 mM Hepes, pH 8.0, 50 mM MgCl<sub>2</sub>, 0.005% Triton X-114, 100  $\mu$ M D-Ala-D-Ala, 50  $\mu$ M UMtri-L-Lys, 250  $\mu$ M ATP, purified MurF<sub>Sp</sub> and 100  $\mu$ M of each tested compound dissolved in DMSO.

#### 4.1.2. *E. coli* MurF

50 mM Hepes, pH 8.0, 50 mM MgCl<sub>2</sub>, 0.005% Triton X-114, 600  $\mu$ M D-Ala-D-Ala, 100  $\mu$ M UMtri-mDAP, 500  $\mu$ M ATP, purified MurF<sub>Ec</sub> [29] and 100  $\mu$ M of each tested compound dissolved in DMSO.

#### 4.1.3. *S. aureus* MurF

50 mM Hepes, pH 8.0, 20 mM MgCl<sub>2</sub>, 0.005% Triton X-114, 600  $\mu$ M D-Ala-D-Ala, 50  $\mu$ M UMtri-L-Lys, 500  $\mu$ M ATP, purified MurF<sub>Sa</sub> [14] and 100  $\mu$ M of each tested compound dissolved in DMSO.

In all cases, the final concentration of DMSO was 5% (v/v). The mixtures were incubated at 37 °C for 15 min, and then quenched with 100  $\mu$ L Biomol<sup>®</sup> reagent. After 5 min, the absorbance at 650 nm was measured. All of the experiments were run in duplicate. Residual activities (RAs) were calculated with respect to similar assays without the tested compounds and with 5% DMSO. The IC<sub>50</sub> values, which were determined by measuring the residual activities at seven different compound concentrations, represented the concentrations for which the RA was 50%.

### 4.2. Microbiological evaluation

Minimum inhibitory concentrations (MICs) for selected compounds were determined by broth microdilution in Mueller–Hinton broth (MHB), against *S. aureus* SH1000 [30], *S. pneumoniae* R6 [31], and *E. coli* strains 1411, SM1411 (*acrAB* derivative of 1411) [32], AB734 and ES100 (*tolC* derivative of AB734) [33], according to CLSI guidelines [34]. In the case of *S. pneumoniae*, MHB was supplemented with 5% (v/v) lysed horse blood. To assess the impact of outer-membrane permeability on antimicrobial activity against *E. coli*, MICs were also determined against strains 1411 and AB734 in the presence of 4  $\mu$ g/mL polymyxin B nonapeptide (PMBN) [35].

### 4.3. Co-crystallization, diffraction data collection, structure solution and model refinement

Crystals of conformationally closed MurF<sub>Sp</sub> ligase were obtained by co-crystallizing MurF at 288 K with inhibitors **22m** and **22n**. The crystals were obtained using the vapor diffusion method and the hanging drop system in Linbro plates, by mixing drops of 2  $\mu$ L of MurF solution (15 mg/mL purified enzyme, 20 mM HEPES pH 7.4, 200 mM NaCl, 5 mM dithiothreitol and 1 mM **22m** or **22n**) and 2  $\mu$ L of reservoir solution (0.1 M tris sodium citrate pH 5.6, 0.2 M K/Na-tartrate and 2.2 M (NH<sub>4</sub>)<sub>2</sub>SO<sub>4</sub>). The crystals were grown over 7 days. Crystals were flash cooled in liquid nitrogen using Paratone oil as a cryoprotectant. Diffraction data were collected at ID29 and BM14

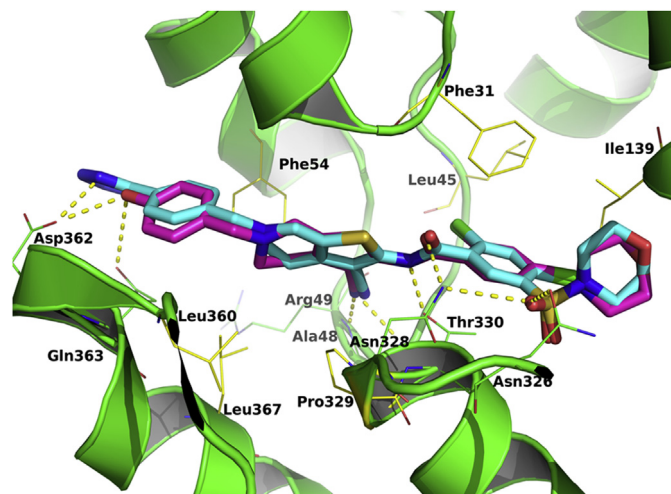


**Fig. 3.** Superposition of co-crystal structures of inhibitors **22m** (cyan) and **22n** (magenta) with MurF<sub>Sp</sub>. MurF active site is colored green and only relevant amino acid residues are shown as lines and colored green if they form hydrogen bond or yellow if they form hydrophobic interactions with the inhibitors. (For interpretation of the references to color in this figure legend, the reader is referred to the web version of this article.)

beamlines of the European Synchrotron Radiation Facility (ESRF, Grenoble, France).

Statistics on diffraction data collection and refinement are summarized in Tables 4 and 5. Datasets were indexed and scaled with XDS program suite [36]. The structures of MurF-**22m** and MurF-**22n** were solved by molecular replacement using MurF (2AM1) as a search model with PHASER 2.3.0 [37]. The models were rebuilt *de novo* to reduce bias using the AutoBuild protocol as implemented in PHENIX 1.8-1069 suite [38] and in ARP/wARP 7.2 [39]. Water molecules were added using the ARP/wARP Solvent protocol. COOT 0.6.2 was used for manual corrections of the model [40], and **22m** and **22n** geometry description was performed with Jligand [41]. Cycles of restrained refinement employing TLS were performed by REFMAC 5.5 [42] as implemented in the CCP4-6.2.0 suite of programs [43]. The stereo chemical quality of the refined models was verified with PROCHECK [44]. A detailed representation of the binding mode of **22m** and **22n** in MurF active site was made by Ligplot [45] and is presented in Fig. 3. Solved structures displayed 99.5 and 99.8% of the non glycine residues in the most favored and allowed regions of the Ramachandran plot. Figures were generated with PyMol (<http://www.pymol.org>).

#### 4.4. Chemistry

All of the chemicals used were obtained from commercial sources (Acros, Aldrich, Alfa Aesar, Fluka and Merck), and were used without further purification. Solvents were used without purification or drying, unless otherwise stated. Reactions were monitored using analytical thin-layer chromatography plates (Merck, silica gel 60 F<sub>254</sub>, 0.25 mm), and the compounds were visualized with ultraviolet light and ninhydrin or bromocresol green. Silica gel grade 60 (particle size 0.040–0.063 mm; Merck, Germany) was used for flash column chromatography. <sup>1</sup>H and <sup>13</sup>C NMR spectra were recorded on a Bruker AVANCE III 400 MHz spectrometer in CDCl<sub>3</sub>, DMSO-d<sub>6</sub>, acetone-d<sub>6</sub> or pyridine-d<sub>5</sub>, with TMS as the internal

**Table 4**  
Data collection, molecular replacement and structure refinement statistics **22m**.

<b>Data collection</b>	
X-ray source	BM14
Detector	MARCCD 225
Wavelength (Å)	0.978
Scan-range (deg)	90
Oscillation (deg)	1.0
Space group	P6 <sub>1</sub> 22
Cell dimensions <i>a</i> , <i>b</i> , <i>c</i> (Å)	116.2, 116.6, 160.3
Mosaicity (°)	0.110
Resolution (Å) (last shell)	1.84 (1.84–1.95)
No. observed/unique reflections	290,140/52,244
Completeness (%) (last shell)	93.3 (83.1)
<i>R</i> <sub>sym</sub> (last shell)	4.3 (52.1)
<i>I</i> / <i>σ</i> ( <i>I</i> ) (last shell)	37.6 (3.5)
Wilson plot <i>B</i> factor (Å <sup>2</sup> )	32.28
<b>Molecular replacement</b>	
Mol/ASU	1
Phaser LLG	2308
<b>Refinement</b>	
<i>R</i> <sub>work</sub> / <i>R</i> <sub>free</sub> (%)	22.41/25.52
No. of atoms (protein/water)	3577/299
Mean <i>B</i> factor (Å <sup>2</sup> )	37.49
Compound <b>22m</b> mean <i>B</i> factor (Å <sup>2</sup> )	29.86
Rmsd bonds (Å)	0.012
Rmsd angles (deg)	1.667
Residues in most favored/allowed region of Ramachandran plot (%)	99.5
Protein Data Bank entry	3zm6

**Table 5**  
Data collection, molecular replacement and structure refinement statistics **22n**.

<b>Data collection</b>	
X-ray source	ID29
Detector	Pilatus 6M
Wavelength (Å)	0.979
Scan-range (deg)	200
Oscillation (deg)	0.25
Space group	P6 <sub>1</sub> 22
Cell dimensions <i>a</i> , <i>b</i> , <i>c</i> (Å)	119.2, 119.2, 160.7
Mosaicity (°)	0.502
Resolution (Å) (last shell)	2.94 (2.94–3.11)
No. observed/unique reflections	87,684/13,459
Completeness (%) (last shell)	89.8 (85.3)
<i>R</i> <sub>sym</sub> (last shell)	3.9 (48.9)
<i>I</i> / <i>σ</i> ( <i>I</i> ) (last shell)	46.0 (9.0)
Wilson plot <i>B</i> factor (Å <sup>2</sup> )	76.16
<b>Molecular replacement</b>	
Mol/ASU	1
Phaser LLG	2265
<b>Refinement</b>	
<i>R</i> <sub>work</sub> / <i>R</i> <sub>free</sub> (%)	22.48/30.30
No. of atoms (protein/water)	3527/46
Mean <i>B</i> factor (Å <sup>2</sup> )	95.75
Compound <b>22n</b> mean <i>B</i> factor (Å <sup>2</sup> )	86.79
Rmsd bonds (Å)	0.009
Rmsd angles (deg)	1.353
Residues in most favored/allowed region of Ramachandran plot (%)	99.8
Protein Data Bank entry	3zm5

standard. Mass spectra were obtained with a VG-Analytical Auto-spec Q mass spectrometer (Centre for Mass Spectrometry, Institute Jožef Stefan, Ljubljana). Infrared spectra were recorded on a Perkin–Elmer FTIR 1600 spectrometer. Melting points were determined using a Reichert hot-stage microscope, and are uncorrected. Microanalyses were performed on a 240 C, Perkin–Elmer elemental analyzer. Analyses indicated by the symbols of the elements were within 0.4% of the theoretical values. HPLC analyses were performed on an Agilent Technologies HP 1100 instrument with a G1365B UV–VIS detector (220 and 254 nm), using a Luna C18 column (4.6 × 250 mm) at a flow rate of 1 mL/min. In method A the eluant was a mixture of 0.1% TFA in water (A) and acetonitrile (B). The gradient was 40% B to 90% B in 20 min. In method B the eluent was a mixture of water (A) and acetonitrile (B). The gradient was 10% B to 90% B in 20 min. The purity of the tested compounds was established to be ≥95%.

#### 4.5. General procedure for synthesis of compounds **7a–c**

To a solution of **6** (2 g, 14.2 mmol) in DMSO (10 mL), K<sub>2</sub>CO<sub>3</sub> (2.49 g, 18.05 mmol) and the corresponding aryl fluoride (12.9 mmol) were added, and the reaction mixture was stirred at 120 °C for 16 h. The mixture was cooled to room temperature, poured into water (50 mL), and the yellow precipitate was filtered off.

##### 4.5.1. 4-(1,4-Dioxo-8-azaspiro[4.5]decan-8-yl)benzonitrile (**7a**)

Yield = 98%; pale yellow solid; mp 129–131 °C (lit. [46], mp 132–133 °C): <sup>1</sup>H NMR (400 MHz, DMSO-d<sub>6</sub>): δ 1.65 (t, *J* = 5.8 Hz, 4H, 2 × C–CH<sub>2</sub>–CH<sub>2</sub>–N), 3.46 (t, *J* = 5.6 Hz, 4H, 2 × C–CH<sub>2</sub>–CH<sub>2</sub>–N), 3.9 (s, 4H, O–CH<sub>2</sub>–CH<sub>2</sub>–O), 7.03 (d, *J* = 9.0 Hz, 2H, 2 × Ar–H), 7.55 (d, *J* = 9.0 Hz, 2H, 2 × Ar–H) ppm.

#### 4.6. General procedure for synthesis of compounds **8a–c**

To a solution of **7a–c** (3 g) in THF (50 mL), 10% H<sub>2</sub>SO<sub>4</sub> was added (50 mL), and the reaction mixture was stirred at room temperature

for 48 h. THF was evaporated, and the water phase was treated with saturated aqueous NaHCO<sub>3</sub> and extracted with CH<sub>2</sub>Cl<sub>2</sub> (3 × 30 mL). The combined organic phases were washed with water (40 mL) and then brine (40 mL), and dried. CH<sub>2</sub>Cl<sub>2</sub> was evaporated to obtain products **8a–c**.

#### 4.6.1. 4-(4-Oxopiperidin-1-yl)benzonitrile (**8a**)

Yield = 78%; pale yellow solid; mp 92–94 °C (lit. [46], mp 98–100 °C); <sup>1</sup>H NMR (400 MHz, CDCl<sub>3</sub>) δ 2.56 (t, *J* = 6.2 Hz, 4H, 2 × CH<sub>2</sub>–CO), 3.72 (t, *J* = 6.1 Hz, 4H, 2 × N–CH<sub>2</sub>), 6.88 (d, *J* = 9.0 Hz, 2H, 2 × Ar–H), 7.52 (d, *J* = 9.0 Hz, 2H, 2 × Ar–H) ppm.

#### 4.7. General procedure for synthesis of compounds **9a–g**

To a solution of ketone (**8a–c**, **10**, **12e–f** or **14**) (25 mmol) and malononitrile (1.65 g, 25 mmol) in EtOH (50 mL), sulfur (0.88 g, 27.5 mmol) and morpholine (4.35 mL, 50 mmol) were added, and the mixture was stirred at reflux for 2 h. The reaction mixture was cooled to room temperature and the orange solid was collected by filtration and washed with cold EtOH.

#### 4.7.1. 2-Amino-6-(4-cyanophenyl)-4,5,6,7-tetrahydrothieno[2,3-*c*]pyridine-3-carbonitrile (**9a**)

Yield = 82%, orange crystals; mp 224–226 °C; <sup>1</sup>H NMR (400 MHz, CDCl<sub>3</sub>): δ 2.69–2.73 (m, 2H, CH<sub>2</sub>–CH<sub>2</sub>–N), 3.70 (t, *J* = 5.7 Hz, 2H, CH<sub>2</sub>–CH<sub>2</sub>–N), 4.28 (t, *J* = 1.7 Hz, N–CH<sub>2</sub>–Ar), 4.70 (bs, 2H, NH<sub>2</sub>), 6.86 (d, *J* = 9.0 Hz, 2H, 2 × Ar–H), 7.50 (d, *J* = 9.0 Hz, 2H, 2 × Ar–H) ppm. <sup>13</sup>C NMR (DMSO-*d*<sub>6</sub>, 400 MHz): δ 23.41, 43.97, 45.31, 82.60, 98.18, 113.84, 114.16, 115.81, 120.03, 130.40, 133.43, 152.31, 163.75 ppm. ESI-HRMS *m/z* calcd. for [M + (H)]<sup>+</sup> 281.0852, found 281.0861. IR (KBr)  $\nu_{\max}$  3725, 3406, 3317, 3223, 2838, 2439, 2211, 1899, 1644, 1606, 1533, 1514, 1464, 1419, 1390, 1353, 1300, 1246, 1224, 1179, 1132, 1038 cm<sup>−1</sup>. Anal. calcd. for C<sub>28</sub>H<sub>28</sub>Cl<sub>2</sub>N<sub>4</sub>O<sub>7</sub>S<sub>2</sub>: C, 50.38; H, 4.23; N, 8.39. Found C, 50.14; H, 4.02; N, 8.17.

#### 4.7.2. 4-(4-Methoxyphenyl)cyclohexanone (**12e**)

To a mixture of **11** (1.7 g, 8.94 mmol) and Cs<sub>2</sub>CO<sub>3</sub> (4.37 g, 13.4 mmol) in acetone (20 mL), MeI was added (7.84 mL, 126 mmol) dropwise. The reaction mixture was refluxed for 1 h. The solvent was evaporated, and water (30 mL) was added to the crude product. The water phase was extracted with CH<sub>2</sub>Cl<sub>2</sub> (3 × 30 mL), the combined organic phases were dried with Na<sub>2</sub>SO<sub>4</sub>, and the solvent evaporated under reduced pressure. The solid obtained was purified by chromatography. Yield = 93%; white needles; mp = 78–79 °C (lit [47] 74 °C); <sup>1</sup>H NMR (400 MHz, CDCl<sub>3</sub>): δ 1.88–1.99 (m, 2H, CH–CH<sub>2</sub>–CH<sub>2</sub>–CO), 2.20–2.24 (m, 2H, CH–CH<sub>2</sub>–CH<sub>2</sub>–CO), 2.51–2.55 (m, 4H, CH<sub>2</sub>–CO–CH<sub>2</sub>), 3.01 (tt, *J*<sub>1</sub> = 11.9, *J*<sub>2</sub> = 2.9 Hz, 1H, CH), 3.82 (s, 3H, O–CH<sub>3</sub>), 6.89 (d, *J* = 8.6 Hz, 2H, 2 × Ar–H), 7.19 (d, *J* = 8.6 Hz, 2H, 2 × Ar–H) ppm.

#### 4.7.3. 4-(4-Oxocyclohexyl)phenyl acetate (**12f**)

To a solution of **11** (5 g, 26.3 mmol) in pyridine (15 mL), Ac<sub>2</sub>O (10 mL) was added dropwise. The reaction mixture was stirred at room temperature for 18 h. Then water (100 mL) was added and the pH was adjusted to 1 with HCl (37%). The water was extracted with EtOAc (4 × 50 mL), the organic phase was washed with brine (100 mL), dried (Na<sub>2</sub>SO<sub>4</sub>), and evaporated under reduced pressure. The crude product was purified by flash chromatography. Yield = 58%; white needles; mp 108–111 °C; <sup>1</sup>H NMR (400 MHz, CDCl<sub>3</sub>): δ 1.87–1.97 (m, 2H, CH–CH<sub>2</sub>–CH<sub>2</sub>–CO), 2.19–2.25 (m, 2H, CH–CH<sub>2</sub>–CH<sub>2</sub>–CO), 2.30 (s, 3H, CH<sub>3</sub>–CO), 2.49–2.53 (m, 4H, CH<sub>2</sub>–CO–CH<sub>2</sub>), 3.03 (tt, *J*<sub>1</sub> = 12.4, *J*<sub>2</sub> = 3.4 Hz, 1H, CH), 7.04 (d, *J* = 8.4 Hz, 2H, 2 × Ar–H), 7.25 (d, *J* = 8.4 Hz, 2H, 2 × Ar–H) ppm. <sup>13</sup>C NMR (400 MHz, CDCl<sub>3</sub>): δ 21.16, 34.01, 41.32, 42.21, 121.64, 127.67, 142.32,

149.18, 169.67, 211.00 ppm. ESI HRMS *m/z* calcd. for [M + (H)]<sup>+</sup> 233.1178, found 233.1169. IR (KBr)  $\nu_{\max}$ : 3396, 3051, 2963, 2931, 2865, 1749, 1710, 1509, 1465, 1432, 1419, 1370, 1348, 1331, 1219, 1197, 1165, 1109, 1042, 1015 cm<sup>−1</sup>. Anal. calcd. for C<sub>14</sub>H<sub>16</sub>O<sub>3</sub> × 0.1H<sub>2</sub>O: C, 71.84; H, 6.98. Found C, 71.92; H, 6.95.

#### 4.7.4. Synthesis of tert-butyl 4-oxopiperidine-1-carboxylate (**14**)

To a solution of **13** (15 g, 97.6 mmol) in a mixture of dioxane and water (4/1, 200 mL), TEA (33.8 mL, 0.244 mol) was added. To this mixture Boc<sub>2</sub>O (21.3 g, 146 mmol) was added portion-wise. The mixture was stirred overnight at room temperature. The solvent was evaporated, and the residue dissolved in 5% citric acid (100 mL) and extracted with CH<sub>2</sub>Cl<sub>2</sub> (3 × 75 mL). The combined organic phases were washed with brine (100 mL) and dried with Na<sub>2</sub>SO<sub>4</sub>. The solvent was evaporated and the crude product was recrystallized from cyclohexane to obtain pure compound **14**. Yield: 89%; white needles; mp 73–75 °C (lit. [48] 72 °C); <sup>1</sup>H NMR (400 MHz, CDCl<sub>3</sub>): δ 1.50 (s, 9H, 3 × CH<sub>3</sub>), 2.44 (t, *J* = 6.5 Hz, 4H, 2 × CH<sub>2</sub>–N), 3.72 (t, *J* = 6.1 Hz, 4H, 2 × CH<sub>2</sub>–CO) ppm.

#### 4.7.5. 2,4-Dichloro-5-(chlorosulfonyl)benzoic acid (**16**)

To a cooled (0 °C) chlorosulfonic acid (10.5 mL, 157 mmol), compound **15** (5 g, 26.2 mmol) was added portion-wise. The reaction mixture was subsequently heated to 140 °C and stirred for 16 h. The reaction mixture was cooled to room temperature, poured into crushed ice, and the white solid formed was collected by filtration. Yield = 77%; white solid; mp 182–184 °C (lit. [49] 183–185 °C); <sup>1</sup>H NMR (400 MHz, DMSO-*d*<sub>6</sub>): δ 7.66 (s, 1H, Ar–H), 8.29 (s, 1H, Ar–H), 13.93 (s, 1H, COOH) ppm.

#### 4.8. General procedure for synthesis of compounds **17a–h**

To a solution of **16** (3 g, 10.4 mmol) in CH<sub>2</sub>Cl<sub>2</sub> (20 mL), TEA was added (3.4 mL, 26 mmol) and the mixture was cooled to 0 °C. The corresponding secondary amine (11.4 mmol) was added slowly and the mixture was stirred overnight at room temperature. Then 1 M HCl was added (20 mL) and it was extracted with CH<sub>2</sub>Cl<sub>2</sub> (3 × 30 mL). The combined organic phases were washed with brine (50 mL), dried (Na<sub>2</sub>SO<sub>4</sub>), and evaporated under reduced pressure. The crude product was purified by flash chromatography.

#### 4.8.1. 2,4-Dichloro-5-(thiomorpholin-4-ylsulfonyl)benzoic acid (**17a**)

Yield = 8%; white crystals; mp 176–178 °C; <sup>1</sup>H NMR (400 MHz, CDCl<sub>3</sub>): δ 2.68 (bs, 4H, CH<sub>2</sub>–S–CH<sub>2</sub>), 3.58 (bs, 4H, CH<sub>2</sub>–N–CH<sub>2</sub>), 7.62 (s, 1H, Ar–H), 8.59 (s, 1H, Ar–H) ppm, COOH exchanged. <sup>13</sup>C NMR (400 MHz, Py-*d*<sub>5</sub>): δ 29.69, 50.00, 136.01, 136.42, 136.73, 137.37, 137.59, 140.43, 169.72 ppm. ESI HRMS *m/z* calcd. for [M + (H)]<sup>+</sup> 355.9585, found 355.9576. IR (KBr)  $\nu_{\max}$ : 3444, 2903, 1694, 1580, 1544, 1398, 1353, 1289, 1251, 1166, 1127, 1085, 1068, 1021 cm<sup>−1</sup>. Anal. calcd. for C<sub>11</sub>H<sub>11</sub>Cl<sub>2</sub>NO<sub>4</sub>S<sub>2</sub>: C, 37.09; H, 3.11; N, 3.93. Found C, 37.00; H, 2.95; N, 3.82.

#### 4.9. General procedure for synthesis of compounds **18a–n**

To a solution of **17a–h** (2.78 g, 8.17 mmol) in anhydrous CH<sub>2</sub>Cl<sub>2</sub> (30 mL), catalytic amounts of DMF and (COCl)<sub>2</sub> (2.1 mL, 24.5 mmol) were added drop-wise, and the mixture was stirred for 0.5 h at room temperature. The solvent was evaporated to dryness and the residue was dissolved in CH<sub>2</sub>Cl<sub>2</sub> (20 mL), **9a–g** (2.05 g, 7.35 mmol) and pyridine (2 mL, 24.5 mmol) were added drop-wise, and the mixture was stirred overnight at room temperature. The reaction mixture was washed with 1 M HCl (30 mL), saturated aqueous NaHCO<sub>3</sub> (30 mL) and brine (30 mL), and dried (Na<sub>2</sub>SO<sub>4</sub>), and the solvent evaporated under reduced pressure. The crude product was purified by flash chromatography.

#### 4.9.1. 2,4-Dichloro-N-(3-cyano-4,5,6,7-tetrahydro-1-benzothiophen-2-yl)-5-(thiomorpholin-4-ylsulfonyl)benzamide (**18a**)

Yield = 25%; pale orange crystals; mp 252–254 °C;  $^1\text{H}$  NMR (400 MHz,  $\text{CDCl}_3$ ):  $\delta$  1.84–1.89 (m, 4H,  $\text{C}-\text{CH}_2-\text{CH}_2-\text{CH}_2-\text{CH}_2-\text{C}$ ), 2.61 (t,  $J = 4.8$  Hz, 2H,  $\text{C}-\text{CH}_2-\text{CH}_2-\text{CH}_2-\text{CH}_2-\text{C}$ ), 2.69–2.71 (m, 6H,  $\text{C}-\text{CH}_2-\text{CH}_2-\text{CH}_2-\text{CH}_2-\text{C} + \text{CH}_2-\text{S}-\text{CH}_2$ ), 3.62 (t,  $J = 4.8$  Hz, 4H,  $\text{CH}_2-\text{N}-\text{CH}_2$ ), 7.69 (s, 1H, Ar-H), 8.54 (s, 1H, Ar-H), 9.58 (s, 1H, NH) ppm.  $^{13}\text{C}$  NMR (400 MHz,  $\text{CDCl}_3$ ):  $\delta$  22.04, 23.01, 23.98, 24.03, 27.54, 47.78, 95.07, 114.05, 129.79, 130.98, 131.56, 133.74, 134.26, 135.64, 135.91, 136.56, 145.50, 160.09 ppm. ESI HRMS  $m/z$  calcd. for  $[\text{M} + (\text{H})]^+$  516.0044, found 516.0050. IR (KBr)  $\nu_{\text{max}}$ : 3448, 3303, 3094, 2944, 2914, 2860, 2214, 1694, 1573, 1549, 1449, 1357, 1342, 1329, 1292, 1281, 1264, 1153, 1118, 1083, 1068, 1024  $\text{cm}^{-1}$ . Anal. calcd. for  $\text{C}_{20}\text{H}_{19}\text{Cl}_2\text{N}_3\text{O}_3\text{S}_3$ : C, 46.51; H, 3.71; N, 8.14. Found: C, 46.71; H, 3.58; N, 8.23.

#### 4.10. Synthesis of compounds **19d–e**

To a solution of **18d–e** (0.150 g, 0.263 mmol) in a mixture of dioxane and water (1/1, 5 mL), KOH (0.06 g, 1.05 mmol) was added. The reaction mixture was stirred at room temperature for 2 h. Dioxane was then evaporated under reduced pressure and the remaining water was acidified to pH 1. The precipitate obtained was collected by filtration.

##### 4.10.1. 1-(2,4-Dichloro-5-(3-cyano-4,5,6,7-tetrahydrobenzo[b]thiophen-2-ylcarbamoyl)phenylsulfonyl) piperidine-3-carboxylic acid (**19d**)

Yield = 84%; white solid; mp = 278–280 °C;  $^1\text{H}$  NMR (400 MHz,  $\text{DMSO}-d_6$ ):  $\delta$  1.47–1.56 (m, 2H,  $\text{N}-\text{CH}_2-\text{CH}_2-\text{CH}_2-\text{CH}$ ), 1.71–1.78 (m, 5H,  $\text{C}-\text{CH}_2-\text{CH}_2-\text{CH}_2-\text{CH}_2-\text{C} + \text{CH}_A\text{H}_B-\text{CH}$ ), 1.90–1.94 (m, 1H,  $\text{CH}_A\text{H}_B-\text{CH}$ ), 2.65 (bs, 2H,  $\text{C}-\text{CH}_2-\text{CH}_2-\text{CH}_2-\text{CH}_2-\text{C}$ ), 2.94 (t,  $J = 9.7$  Hz,  $\text{N}-\text{CH}_A\text{H}_B-\text{CH}_2-\text{CH}_2-\text{CH}$ ), 3.04 (t,  $J = 11.0$  Hz,  $\text{N}-\text{CH}_A\text{H}_B-\text{CH}_2-\text{CH}_2-\text{CH}$ ), 3.52 (d,  $J = 12.6$  Hz,  $\text{N}-\text{CH}_A\text{CH}_B-\text{CH}$ ), 3.72 (dd,  $J_1 = 12.6$ ,  $J_2 = 3.7$  Hz,  $\text{N}-\text{CH}_A\text{CH}_B-\text{CH}$ ), 8.11 (s, 1H, Ar-H), 8.16 (s, 1H, Ar-H), 12.35 (s, 1H, NH), 12.53 (bs, 1H, COOH) ppm.  $^{13}\text{C}$  NMR (400 MHz,  $\text{DMSO}-d_6$ ):  $\delta$  21.70, 22.60, 23.45, 23.57, 23.90, 25.75, 40.43, 45.47, 46.84, 94.43, 114.04, 128.36, 131.30, 131.74, 132.78, 133.37, 133.87, 134.83, 135.79, 145.64, 162.32, 173.72 ppm. ESI-HRMS  $m/z$  calcd. for  $[\text{M} + (\text{H})]^+$  542.0378, found 542.0395. IR (KBr)  $\nu_{\text{max}}$ : 3854, 3317, 3097, 2941, 2860, 2361, 2215, 1833, 1702, 1672, 1570, 1552, 1448, 1337, 1286, 1255, 1218, 1171, 1157, 1136, 1081, 1052, 1030  $\text{cm}^{-1}$ . Anal. calcd. for  $\text{C}_{22}\text{H}_{21}\text{Cl}_2\text{N}_3\text{O}_5\text{S}_2 \times 0.6\text{H}_2\text{O}$ : C, 47.76; H, 4.04; N, 7.59. Found: C, 47.50; H, 3.65; N, 7.32.

##### 4.10.2. 2,4-Dichloro-N-(3-cyano-4,5,6,7-tetrahydrobenzo[b]thiophen-2-yl)-5-((4-hydroxypiperidin-1-yl)sulfonyl)benzamide (**20**)

To a solution of **18f** (0.180 g, 0.351 mmol) in a mixture of EtOH and  $\text{CH}_2\text{Cl}_2$  (1/1, 10 mL),  $\text{NaBH}_4$  (0.027 g, 0.703 mmol) was added and the reaction mixture was stirred at room temperature for 3 h. The solvent was evaporated to dryness, the crude residue was dissolved in EtOAc (20 mL), washed with saturated aqueous  $\text{NaHCO}_3$  (20 mL) and brine (20 mL), dried with  $\text{Na}_2\text{SO}_4$ , and evaporated under reduced pressure. The solid was purified by flash chromatography. Yield = 67%; pale yellow crystals; mp 217–219 °C;  $^1\text{H}$  NMR (400 MHz,  $\text{CDCl}_3$ ):  $\delta$  1.54 (d,  $J = 3.42$  Hz, 1H,  $\text{CH}-\text{OH}$ ), 1.60–1.66 (m, 2H,  $\text{CH}_2-\text{CH}-\text{CH}_2$ ), 1.83–1.88 (m, 4H,  $\text{C}-\text{CH}_2-\text{CH}_2-\text{CH}_2-\text{CH}_2-\text{C}$ ), 1.90–1.97 (m, 2H,  $\text{CH}_2-\text{CH}-\text{CH}_2$ ), 2.60–2.62 (t,  $J = 4.8$  Hz, 2H,  $\text{C}-\text{CH}_2-\text{CH}_2-\text{CH}_2-\text{CH}_2-\text{C}$ ), 2.68–2.70 (t,  $J = 4.8$  Hz, 2H,  $\text{C}-\text{CH}_2-\text{CH}_2-\text{CH}_2-\text{CH}_2-\text{C}$ ), 3.16–3.22 (m, 2H,  $\text{CH}_2-\text{N}-\text{CH}_2$ ), 3.56–3.61 (m, 2H,  $\text{CH}_2-\text{N}-\text{CH}_2$ ), 3.88–3.92 (m, 1H, CH), 7.68 (s, 1H, Ar-H), 8.52 (s, 1H, Ar-H), 9.62 (s, 1H,  $\text{NH}-\text{CO}$ ) ppm.  $^{13}\text{C}$  NMR (400 MHz,  $\text{CDCl}_3$ ):  $\delta$  22.04, 23.02, 23.99, 24.04, 33.64, 42.88, 66.95, 95.16, 114.08, 129.79, 130.69, 131.56, 133.80, 134.32, 135.55, 136.03, 136.64, 145.41, 160.04 ppm. ESI HRMS  $m/z$  calcd. for

$[\text{M} + (\text{H})]^+$  514.0429, found 514.0416. IR (KBr)  $\nu_{\text{max}}$ : 3260, 3085, 2931, 2215, 1678, 1572, 1447, 1406, 1329, 1286, 1259, 1157, 1077, 1039  $\text{cm}^{-1}$ . Anal. calcd. for  $\text{C}_{21}\text{H}_{21}\text{Cl}_2\text{N}_3\text{O}_4\text{S}_2$ : C, 49.03; H, 4.11; N, 8.17. Found: C, 48.79; H, 4.14; N, 7.78.

##### 4.10.3. 3-Cyano-2-(2,4-dichloro-5-(morpholinosulfonyl)benzamido)-4,5,6,7-tetrahydrothieno[2,3-c]pyridin-6-ium 2,2,2-trifluoroacetate (**21**)

To a solution of **18i** (1 g, 1.66 mmol) in  $\text{CH}_2\text{Cl}_2$  (20 mL),  $\text{CF}_3\text{COOH}$  (5 mL) or HCl in EtOH (2 M, 10 mL) was added and stirred at room temperature for 2 h. The solvent was evaporated under reduced pressure and the residue was recrystallized from EtOH to obtain **21**. Yield = 94%; white powder; mp 268–270 °C;  $^1\text{H}$  NMR (400 MHz,  $\text{DMSO}-d_6$ ):  $\delta$  2.75 (t,  $J = 5.1$  Hz, 2H,  $\text{CH}_2$ ), 3.18 (t,  $J = 4.5$  Hz, 4H,  $2 \times \text{CH}_2-\text{N}-\text{morpholine}$ ), 3.63 (t,  $J = 4.4$  Hz, 4H,  $2 \times \text{CH}_2-\text{O}-\text{morpholine}$ ), 4.14 (s, 2H,  $\text{CH}_2-\text{N}$ ), 7.88 (s, 1H, Ar-H), 8.30 (s, 1H, Ar-H), 8.94 (bs, 1H, NH) ppm,  $\text{CH}_2-\text{CH}_2-\text{N}$  covered with water from DMSO,  $\text{NH}_2$  exchanged.  $^{13}\text{C}$  NMR (400 MHz,  $\text{DMSO}-d_6$ ):  $\delta$  21.13, 40.91, 41.72, 45.53, 65.68, 90.63, 105.17, 114.89, 117.24, 126.65, 130.75, 132.93, 132.96, 133.14, 136.50, 138.61, 165.97 ppm. ESI-HRMS  $m/z$  calcd. for  $[\text{M} + (\text{H})]^+$  501.0225, found 501.0223. IR (KBr)  $\nu_{\text{max}}$ : 3448, 3064, 2970, 2921, 2867, 2738, 2617, 2481, 2223, 1698, 1678, 1583, 1566, 1471, 1454, 1434, 1390, 1367, 1341, 1322, 1293, 1262, 1246, 1193, 1157, 1134, 1120, 1086, 1018  $\text{cm}^{-1}$ . Anal. calcd. for  $\text{C}_{19}\text{H}_{18}\text{Cl}_2\text{N}_4\text{O}_4\text{S}_2 \times \text{CF}_3\text{COOH}$ : C, 40.98; H, 3.11; N, 9.10. Found: C, 41.04; H, 3.13; N, 8.83.

#### 4.11. General procedures for synthesis of compounds **22a–w**

Method A: To a solution of **21** (0.100 g, 0.186 mmol) in DMF (3 mL),  $\text{K}_2\text{CO}_3$  (0.100 g, 0.740 mmol) was added. After 10 min of stirring at room temperature, the corresponding benzyl bromide was added (0.195 mmol). The reaction mixture was stirred overnight at room temperature. DMF was then evaporated, the crude residue was dissolved in EtOAc (20 mL) and washed with water ( $3 \times 10$  mL), brine (10 mL) and dried with  $\text{Na}_2\text{SO}_4$ . The yellow solid was purified by flash chromatography.

Method B: To a solution of **21** (0.150 g, 0.244 mmol) in THF (10 mL), the corresponding benzaldehyde (0.268 mmol),  $\text{CH}_3\text{COOH}$  (0.014 mL, 0.244 mmol) and  $\text{Na}(\text{OAc})_3\text{BH}$  (0.103 g, 4.88 mmol) were added, and the reaction mixture was stirred overnight at room temperature. To quench the reaction, saturated aqueous  $\text{NaHCO}_3$  (10 mL) was used, and the water phase was extracted with EtOAc ( $3 \times 10$  mL), washed with brine (20 mL) and dried with  $\text{Na}_2\text{SO}_4$ . The crude residue was purified by flash chromatography.

##### 4.11.1. N-(6-Benzyl-3-cyano-4,5,6,7-tetrahydrothieno[2,3-c]pyridin-2-yl)-2,4-dichloro-5-(morpholino sulfonyl)benzamide (**22c**)

Yield = 45%; mp 126–128 °C;  $^1\text{H}$  NMR (400 MHz,  $\text{CDCl}_3$ ):  $\delta$  2.74 (t,  $J = 5.1$  Hz, 2H,  $\text{CH}_2-\text{CH}_2-\text{N}$ ), 2.84 (t,  $J = 5.6$  Hz, 2H,  $\text{CH}_2-\text{CH}_2-\text{N}$ ), 3.31 (t,  $J = 4.7$  Hz, 4H,  $2 \times \text{CH}_2-\text{N}-\text{morpholine}$ ), 3.58 (s, 2H,  $\text{N}-\text{CH}_2$ ), 3.70–3.73 (m, 6H,  $2 \times \text{CH}_2-\text{O}-\text{morpholine} + \text{N}-\text{CH}_2-\text{Bz}$ ), 7.28–7.53 (m, 5H,  $5 \times \text{Ar}-\text{H}$ ), 7.70 (s, 1H, Ar-H), 8.57 (s, 1H, Ar-H), 9.57 (bs, 1H, NH) ppm.  $^{13}\text{C}$  NMR (400 MHz,  $\text{CDCl}_3$ ):  $\delta$  24.26, 46.08, 49.51, 50.83, 61.81, 66.72, 94.86, 113.89, 116.45, 123.76, 127.37, 127.74, 128.74, 129.33, 130.38, 130.94, 134.12, 134.68, 135.89, 136.25, 146.40, 160.30 ppm. ESI-HRMS  $m/z$  calcd. for  $[\text{M} + (\text{H})]^+$  591.0694, found 591.0699. IR (KBr)  $\nu_{\text{max}}$ : 3774, 3320, 2858, 2457, 2212, 1912, 1669, 1582, 1550, 1451, 1358, 1329, 1262, 1172, 1113, 1072  $\text{cm}^{-1}$ . HPLC (method A)  $t_R = 6.181$  min (99.42% at 220 nm, 97.60% at 254 nm).

##### 4.11.2. N-(6-Benzoyl-3-cyano-4,5,6,7-tetrahydrothieno[2,3-c]pyridin-2-yl)-2,4-dichloro-5-(morpholinosulfonyl)benzamide (**23**)

To a solution of **21** (0.100 g, 0.16 mmol) in  $\text{CH}_2\text{Cl}_2$  (5 mL), TEA (0.055 mL, 0.40 mmol) was added. After 10 min benzoyl chloride



(0.028 mL, 0.25 mmol) was added drop-wise. The reaction mixture was stirred for 16 h at room temperature. The mixture was diluted with  $\text{CH}_2\text{Cl}_2$  (20 mL) and washed with water (10 mL), 1 M HCl (10 mL), saturated aqueous  $\text{NaHCO}_3$  (10 mL) and brine (15 mL). The solvent was dried over  $\text{Na}_2\text{SO}_4$  and evaporated under reduced pressure. The crude product was purified by flash chromatography. Yield = 62%; white solid; mp 258–260 °C;  $^1\text{H}$  NMR (400 MHz,  $\text{CDCl}_3$ ):  $\delta$  2.73 (t,  $J$  = 5.5 Hz, 2H,  $\text{N}-\text{CH}_2-\text{CH}_2$ ), 3.23 (t,  $J$  = 4.4 Hz, 4H,  $2 \times \text{CH}_2-\text{N}$ -morpholine), 3.63–3.65 (m, 6H,  $2 \times \text{CH}_2-\text{O}$ -morpholine +  $\text{N}-\text{CH}_2-\text{CH}_2$ ), 4.77 (s, 2H,  $\text{CO}-\text{N}-\text{CH}_2$ ), 7.47–7.52 (m, 5H,  $5 \times \text{Ar}-\text{H}$ ), 8.16 (s, 1H  $\text{Ar}-\text{H}$ ), 8.19 (s, 1H,  $\text{Ar}-\text{H}$ ), 12.53 (bs, 1H, NH) ppm.  $^{13}\text{C}$  NMR (400 MHz,  $\text{DMSO}-d_6$ ):  $\delta$  22.11, 40.82, 44.13, 45.52, 65.73, 93.95, 113.60, 124.74, 126.85, 128.57, 129.27, 129.88, 130.73, 132.03, 132.91, 133.66, 133.98, 135.76, 136.03, 146.84, 162.38, 169.77 ppm. ESI-HRMS  $m/z$  calcd. for  $[\text{M} + (\text{H})]^+$  605.0487, found 605.0496. IR (KBr)  $\nu_{\text{max}}$  3437, 3252, 3088, 2919, 2860, 2216, 1690, 1641, 1576, 1556, 1493, 1433, 1352, 1331, 1288, 1262, 1156, 1116, 1086, 1072, 1050, 1027, 1007  $\text{cm}^{-1}$ . HPLC (method B)  $t_R$  = 12.908 min (98.65% at 220 nm, 100% at 254 nm).

4.11.3. 4-(2-(3-Cyano-2-(2,4-dichloro-5-(morpholinofulfonyl) benzamido)-4,5-dihydrothieno[2,3-*c*]pyridin-6(7H)-yl)ethyl) piperidinium trifluoroacetate (**24**)

To a solution of **22a** (0.2 g, 0.28 mmol) in  $\text{CH}_2\text{Cl}_2$  (3 mL),  $\text{CF}_3\text{COOH}$  was added (1 mL), and the reaction mixture was stirred at room temperature for 3 h. The solvent was evaporated and the product was dried in a desiccator. Yield = 80%; pale yellow solid; mp 128–130 °C;  $^1\text{H}$  NMR (400 MHz,  $\text{DMSO}-d_6$ ):  $\delta$  1.28–1.37 (m, 2H,  $\text{N}-\text{CH}_2-\text{CH}_2-\text{CH}-\text{CH}_2$ ), 1.61–1.71 (m, 3H,  $\text{N}-\text{CH}_2-\text{CH}_2-\text{CH}-\text{CH}_2 + \text{CH}$ ), 1.81–1.85 (m, 2H,  $\text{N}-\text{CH}_2-\text{CH}_2-\text{CH}$ ), 2.81–2.89 (m, 2H), 2.97 (bs, 2H), 3.23–3.30 (m, 8H,  $2 \times \text{CH}_2-\text{N}$ -morpholine +  $2 \times \text{CH}_2$ ), 3.43 (bs, 2H), 3.64 (bs, 4H,  $2 \times \text{CH}_2-\text{O}$ -morpholine), 3.78 (bs, 2H), 4.29 (bs, 2H,  $\text{NH}_2$ ), 8.17 (s, 1H,  $\text{Ar}-\text{H}$ ), 8.21 (s, 1H,  $\text{Ar}-\text{H}$ ), 10.76 (bs, 1H, NH), 12.78 (bs, 1H, COOH).  $^{13}\text{C}$  NMR (400 MHz,  $\text{DMSO}-d_6$ ):  $\delta$  20.96, 28.11, 29.57, 30.81, 42.99, 45.525, 48.35, 48.44, 52.31, 65.74, 93.17, 113.28, 116.71 ( $q$ ,  $J$  = 296.5 Hz), 119.83, 120.01, 132.15, 132.95, 133.42, 133.82, 134.04, 136.03, 148.06, 158.43 ( $q$ ,  $J$  = 33.0 Hz), 162.70 ppm. ESI-HRMS  $m/z$  calcd. for  $[\text{M} + (\text{H})]^+$  612.1285, found 612.1273. IR (KBr)  $\nu_{\text{max}}$  3873, 3406, 2862, 2222, 1682, 1587, 1454, 1340, 1264, 1197, 1020  $\text{cm}^{-1}$ . Anal. calcd. for  $\text{C}_{26}\text{H}_{31}\text{Cl}_2\text{N}_5\text{O}_4\text{S}_2 \times 2.6 \text{ CF}_3\text{COOH}$ : C, 41.22; H, 3.73; N, 7.70. Found: C, 41.00; H, 3.57; N, 7.60.

4.11.4. 2,4-Dichloro-*N*-(3-cyano-6-(3,4-dihydroxybenzyl)-4,5,6,7-tetrahydrothieno[2,3-*c*]pyridin-2-yl)-5-(morpholinofulfonyl) benzamide (**25**)

To a solution of **22q** (0.127 g, 0.179 mmol) in THF (1.5 mL), MeOH (1.5 mL) and NaOMe (30% in MeOH, 0.050 mL) were added. The reaction mixture was stirred at room temperature for 0.5 h. Water was then added (5 mL) and the mixture was acidified with 1 M HCl to pH 7. The water phase was extracted with EtOAc ( $3 \times 10$  mL), the combined organic phases were washed with brine (10 mL) and dried with  $\text{Na}_2\text{SO}_4$ . The solvent was evaporated under reduced pressure and the crude residue was purified by flash chromatography. Yield = 50%; yellow crystals; mp 164–165 °C;  $^1\text{H}$  NMR (400 MHz, acetone- $d_6$ ):  $\delta$  2.68 (t,  $J$  = 5.6 Hz, 2H,  $\text{CH}_2-\text{CH}_2-\text{N}$ ), 2.84 (t,  $J$  = 5.6 Hz, 2H,  $\text{CH}_2-\text{CH}_2-\text{N}$ ), 3.31 (t,  $J$  = 4.7 Hz, 4H,  $2 \times \text{CH}_2-\text{N}$ -morpholine), 3.59 (s, 2H,  $\text{N}-\text{CH}_2$ ), 3.62 (s, 2H,  $\text{N}-\text{CH}_2-\text{Ar}$ ), 3.70 (t,  $J$  = 4.7 Hz, 4H,  $2 \times \text{CH}_2-\text{O}$ -morpholine), 6.71 (dd,  $J_1$  = 8.0,  $J_2$  = 1.9 Hz, 1H,  $\text{Ar}-\text{H}$ ), 6.80 (d,  $J$  = 8.0 Hz, 1H,  $\text{Ar}-\text{H}$ ), 6.91 (d,  $J$  = 1.9 Hz, 1H,  $\text{Ar}-\text{H}$ ), 7.84 (bs, 1H,  $-\text{OH}$ ), 7.94 (s, 1H,  $\text{Ar}-\text{H}$ ), 8.32 (s, 1H,  $\text{Ar}-\text{H}$ ), 11.26 (bs, 1H, NH) ppm.  $^{13}\text{C}$  NMR (400 MHz, pyridine- $d_5$ ):  $\delta$  25.13, 46.64, 50.13, 51.35, 62.08, 67.05, 96.11, 114.93, 116.90, 118.00, 121.24, 128.19, 130.61, 131.50, 133.65, 134.08, 135.11, 135.24, 137.47, 147.12, 147.83, 163.61 ppm (two peaks covered with solvent peaks). ESI-HRMS  $m/z$  calcd. for  $[\text{M} + (\text{H})]^+$  623.0593, found 623.0589. IR (KBr)  $\nu_{\text{max}}$  3853,

3376, 3089, 2856, 2363, 2223, 1832, 1700, 1579, 1560, 1448, 1336, 1285, 1164, 1112, 1084, 1067, 1000  $\text{cm}^{-1}$ . HPLC (method A)  $t_R$  = 3.534 min (97.25% at 220 nm, 98.15% at 254 nm).

## Acknowledgments

We thank OpenEye Scientific Software, Inc. for free academic licenses of their software, and the Ministry of Higher Education, Science and Technology of the Republic of Slovenia for financial support. This study was partially supported by a Young Researcher grant to MH, and a L1-4039 grant to ST and SG, both from the Slovenian Research Agency. We also thank Institute Charles Nodier and Proteus PHC program for supporting our project.

## Appendix A. Supplementary data

Supplementary data related to this article can be found at <http://dx.doi.org/10.1016/j.ejmech.2013.05.013>.

## References

- <http://www.who.int/en/>.
- I. Chopra, C. Schofield, M. Everett, A. O'Neill, K. Miller, M. Wilcox, J.-M. Frère, M. Dawson, L. Czaplewski, U. Urleb, P. Courvalin, Treatment of health-care-associated infections caused by Gram-negative bacteria: a consensus statement, *Lancet Infect. Dis.* (2008) 133–139.
- P. Fernandes, Antibacterial discovery and development – the failure of success? *Nat. Biotechnol.* 24 (2006) 1497–1503.
- D.J. Payne, M.N. Gwynn, D.J. Holmes, D.L. Pompliano, Drugs for bad bugs: confronting the challenges of antibacterial discovery, *Nat. Rev. Drug Discov.* 6 (2007) 29–40.
- D.W. Green, The bacterial cell wall as a source of antibacterial targets, *Expert Opin. Ther. Target* 6 (2002) 1–20.
- A.H. Katz, C.E. Caufield, Structure-based design approaches to cell wall biosynthesis inhibitors, *Curr. Pharm. Des.* 9 (2003) 857–866.
- W. Vollmer, D. Blanot, M.A. De Pedro, Peptidoglycan structure and architecture, *FEMS Microbiol. Rev.* 32 (2008) 149–167.
- A. Gautam, R. Vyas, R. Tewari, Peptidoglycan biosynthesis machinery: a rich source of drug targets, *Crit. Rev. Biotechnol.* 31 (2011) 295–336.
- T.D.H. Bugg, D. Braddick, C.G. Dowson, D.I. Roper, Bacterial cell wall assembly: still an attractive antibacterial target, *Trends Biotechnol.* 29 (2011) 167–173.
- F.M. Kahan, J.S. Kahan, P.J. Cassidy, H. Kropp, The mechanism of action of fosfomycin (phosphonomycin), *Ann. N. Y. Acad. Sci.* 235 (1974) 364–386.
- F.C. Neuhaus, J.L. Lynch, The enzymatic synthesis of  $\text{D}$ -alanyl- $\text{D}$ -alanine. III. On the inhibition of  $\text{D}$ -alanyl- $\text{D}$ -alanine synthetase by the antibiotic  $\text{D}$ -cycloserine, *Biochemistry* 3 (1964) 471–480.
- A. El Zoeiby, F. Sanschagrin, R.C. Levesque, Structure and function of the Mur enzymes: development of novel inhibitors, *Mol. Microbiol.* 47 (2003) 1–12.
- H. Barreateau, A. Kovač, A. Boniface, M. Sova, S. Gobec, D. Blanot, Cytoplasmic steps of peptidoglycan biosynthesis, *FEMS Microbiol. Rev.* 32 (2008) 168–207.
- D. Patin, A. Boniface, A. Kovač, M. Hervé, S. Dementin, H. Barreateau, D. Mengin-Lecreulx, D. Blanot, Purification and biochemical characterization of Mur ligases from *Staphylococcus aureus*, *Biochimie* 92 (2010) 1793–1800.
- J. van Heijenoort, Recent advances in the formation of the bacterial peptidoglycan monomer unit, *Nat. Prod. Rep.* 18 (2001) 503–519.
- K.L. Longenecker, G.F. Stamper, P.J. Hajduk, E.H. Fry, C.G. Jakob, J.E. Harlan, R. Edalji, D.M. Bartley, K.A. Walter, L.R. Solomon, T.F. Holzman, Y.G. Gu, C.G. Lerner, B.A. Beutel, V.S. Stoll, Structure of MurF from *Streptococcus pneumoniae* co-crystallized with a small molecule inhibitor exhibits inter-domain closure, *Protein Sci.* 14 (2005) 3039–3047.
- R.G. Sobral, A.M. Ludovice, H. de Lencastre, A. Tomasz, Role of *murF* in cell wall biosynthesis: isolation and characterization of a *murF* conditional mutant of *Staphylococcus aureus*, *J. Bacteriol.* 188 (2006) 2543–2553.
- E.J.J. Lugtenberg, A. van Schijndel-van Dam, Temperature-sensitive mutants of *Escherichia coli* K-12 with low activities of the  $\text{L}$ -alanine adding enzyme and the  $\text{D}$ -alanyl- $\text{D}$ -alanine adding enzyme, *J. Bacteriol.* 110 (1972) 35–40.
- E.Z. Baum, S.M. Crespo-Carbone, D. Abbanat, B. Foleno, A. Maden, R. Goldschmidt, K. Bush, Utility of mucopeptide ligase for identification of inhibitors of the cell wall biosynthesis enzyme MurF, *Antimicrob. Agents Chemother.* 50 (2006) 230–236.
- D.J. Miller, S.M. Hammond, D. Anderluzzi, T.D.H. Bugg, Amino-alkylphosphinate inhibitors of  $\text{D}$ -Ala- $\text{D}$ -Ala adding enzyme, *J. Chem. Soc. Perkin Trans. 1* (1998) 131–142.
- K.M. Comess, M.E. Schurdak, M.J. Voorbach, M. Coen, J.D. Trumbull, H. Yang, L. Gao, H. Tang, X. Cheng, C.G. Lerner, J.O. Mccall, D.J. Burns, B.A. Beutel, An ultraefficient affinity-based high-throughput screening process: application to bacterial cell wall biosynthesis enzyme MurF, *J. Biomol. Screen.* 11 (2006) 743–754.



- [22] Y.G. Gu, A.S. Florjancic, R.F. Clark, T. Zhang, C.S. Cooper, D.D. Anderson, C.G. Lerner, J.O. McCall, Y. Cai, C.L. Black-Schaefer, G.F. Stamper, P.J. Hajduk, B.A. Beutel, Structure–activity relationships of novel potent MurF inhibitors, *Bioorg. Med. Chem. Lett.* 14 (2004) 267–270.
- [23] G.F. Stamper, K.L. Longenecker, E.H. Fry, C.G. Jakob, A.S. Florjancic, Y.-G. Gu, D.D. Anderson, C.S. Cooper, T. Zhang, R.F. Clark, Y. Cia, C.L. Black-Schaefer, J. Owen McCall, C.G. Lerner, P.J. Hajduk, B.A. Beutel, V.S. Stoll, Structure-based optimization of MurF inhibitors, *Chem. Biol. Drug Des.* 67 (2006) 58–65.
- [24] S. Turk, A. Kovač, A. Boniface, J.M. Bostock, I. Chopra, D. Blanot, S. Gobec, Discovery of new inhibitors of the bacterial peptidoglycan biosynthesis enzymes MurD and MurF by structure-based virtual screening, *Bioorg. Med. Chem.* 17 (2009) 1884–1889.
- [25] E.Z. Baum, S.M. Crespo-Carbone, A. Klinger, B.D. Folen, I. Turchi, M. Macielag, K. Bush, A MurF inhibitor that disrupts cell wall biosynthesis in *Escherichia coli*, *Antimicrob. Agents Chemother.* 51 (2007) 4420–4426.
- [26] E.Z. Baum, S.M. Crespo-Carbone, B.D. Folen, L.D. Simon, J. Guillemont, M. Macielag, K. Bush, MurF inhibitors with antibacterial activity: effect on muropeptide levels, *Antimicrob. Agents Chemother.* 53 (2009) 3240–3247.
- [27] P.A. Lanzetta, L.J. Alvarez, P.S. Reinach, O.A. Candia, An improved assay for nanomole amounts of inorganic phosphate, *Anal. Biochem.* 100 (1979) 95–97.
- [28] S.L. McGovern, B.T. Helfand, B. Feng, B.K. Shoichet, A specific mechanism of nonspecific inhibition, *J. Med. Chem.* 46 (2003) 4265–4272.
- [29] S. Dementin, A. Bouhss, G. Auger, C. Parquet, D. Mengin-Lecreulx, O. Dideberg, J. van Heijenoort, D. Blanot, Evidence of a functional requirement for a carbamoylated lysine residue in MurD, MurE and MurF synthetases as established by chemical rescue experiments, *Eur. J. Biochem.* 268 (2001) 5800–5807.
- [30] M.J. Horsburgh, J.L. Aish, I.J. White, L. Shaw, J.K. Lithgow, S.J. Foster,  $\sigma^B$  modulates virulence determinant expression and stress resistance: characterization of a functional *rsbU* strain derived from *Staphylococcus aureus* 8325-4, *J. Bacteriol.* 184 (2002) 5457–5467.
- [31] J. Hoskins, W.E. Alborn Jr., J. Arnold, L.C. Blaszcak, S. Burgett, B.S. DeHoff, S.T. Estrem, L. Fritz, D.J. Fu, W. Fuller, C. Geringer, R. Gilmour, J.S. Glass, H. Khoja, A.R. Kraft, R.E. Lagace, D.J. LeBlanc, L.N. Lee, E.J. Lefkowitz, J. Lu, P. Matsushima, S.M. McAhren, M. McHenney, K. McLeaster, C.W. Mundy, T.I. Nicas, F.H. Norris, M. O'Gara, R.B. Peery, G.T. Robertson, P. Rockey, P.M. Sun, M.E. Winkler, Y. Yang, M. Young-Bellido, G. Zhao, C.A. Zook, R.H. Baltz, S.R. Jaskunas, P.R. Rostek Jr., P.L. Skatrud, J.I. Glass, Genome of the bacterium *Streptococcus pneumoniae* strain R6, *J. Bacteriol.* 183 (2001) 5709–5717.
- [32] A.J. O'Neill, J.M. Bostock, A.M. Moita, I. Chopra, Antimicrobial activity and mechanisms of resistance to cephalosporin P1, an antibiotic related to fusidic acid, *J. Antimicrob. Chemother.* 50 (2002) 839–848.
- [33] E. Shapiro, F. Baneyx, Stress-based identification and classification of antibacterial agents: second-generation *Escherichia coli* reporter strains and optimization of detection, *Antimicrob. Agents Chemother.* 46 (2002) 2490–2497.
- [34] National Committee for Clinical Laboratory Standards (NCCLS) Methods for Dilution Antimicrobial Susceptibility Tests for Bacteria that Grow Aerobically, fourth ed. vol. 17, no. 2. Approved standard M7-A4, 1997.
- [35] R.A. Dixon, I. Chopra, Leakage of periplasmic proteins from *Escherichia coli* mediated by polymyxin B nonapeptide, *Antimicrob. Agents Chemother.* 29 (1986) 781–788.
- [36] W. Kabsch, XDS, *Acta Crystallogr. D* 66 (2010) 125–132.
- [37] A.J. McCoy, R.W. Grosse-Kunstleve, P.D. Adams, M.D. Winn, L.C. Storoni, R.J. Read, Phaser crystallographic software, *J. Appl. Crystallogr.* 40 (2007) 658–674.
- [38] P.D. Adams, P.V. Afonine, G. Bunkoczi, V.B. Chen, I.W. Davis, N. Echols, J.J. Headd, L.-W. Hung, G.J. Kapral, R.W. Grosse-Kunstleve, A.J. McCoy, N.W. Moriarty, R. Oeffner, R.J. Read, D.C. Richardson, J.S. Richardson, T.C. Terwilliger, P.H. Zwart, PHENIX: a comprehensive python-based system for macromolecular structure solution, *Acta Crystallogr. D* 66 (2010) 213–221.
- [39] G. Langer, S.X. Cohen, V.S. Lamzin, A. Perrakis, Automated macromolecular model building for X-ray crystallography using ARP/wARP version 7, *Nat. Protoc.* 3 (2008) 1171–1179.
- [40] P. Emsley, K. Cowtan, Coot: model-building tools for molecular graphics, *Acta Crystallogr. D* 60 (2004) 2126–2132.
- [41] A.A. Lebedev, P. Young, M.N. Isupov, O.V. Moroz, A.A. Vagin, G.N. Murshudov, Jligand: a graphical tool for the CCP4 template-restraint library, *Acta Crystallogr. D* 68 (2012) 431–440.
- [42] G.N. Murshudov, P. Skubak, A.A. Lebedev, N.S. Pannu, R.A. Steiner, R.A. Nicholls, M.D. Winn, F. Long, A.A. Vagin, REFMAC5 for the refinement of macromolecular crystal structures, *Acta Crystallogr. D* 67 (2011) 355–367.
- [43] N. Collaborative Computational Project, The CCP4 suite: programs for protein crystallography, *Acta Crystallogr. D* 50 (1994) 760–763.
- [44] R.A. Laskowski, M.W. MacArthur, D.S. Moss, J.M. Thornton, PROCHECK: a program to check the stereochemical quality of protein structures, *J. Appl. Crystallogr.* 26 (1993) 283–291.
- [45] A.C. Wallace, R.A. Laskowski, J.M. Thornton, LIGPLOT: a program to generate schematic diagrams of protein–ligand interactions, *Protein Eng.* 8 (1995) 127–134.
- [46] E.C. Taylor, J.S. Skotnicki, A convenient synthesis of 1-aryl-4-piperidones, *Synthesis* (1981) 606–608.
- [47] A. Friesse, K. Hell-Momeni, I. Zündorf, T. Winckler, T. Dingermann, G. Dannhardt, Synthesis and biological evaluation of cycloalkylidene carboxylic acids as novel effectors of Ras/Raf interaction, *J. Med. Chem.* 45 (2002) 1535–1542.
- [48] V.D. Vitnik, M.D. Ivanović, Ž.J. Vitnik, J.B. Đorđević, Ž.S. Žizak, Z.D. Juranić, I.O. Juranić, One-step conversion of ketones to conjugated acids using bromoform, *Synth. Commun.* 39 (2009) 1457–1471.
- [49] B. Loev, M.M. Goodman, K.M. Snader, R. Tedeschi, E. Macko, Hantzsch-type dihydropyridine hypotensive agents, *J. Med. Chem.* 17 (1974) 956–965.